JOURNAL OF FOOD PROCESS ENGINEERING

D.R. HELDMAN
and
R.P. SINGH
COEDITORS

FOOD & NUTRITION PRESS, INC.

VOLUME 15, NUMBER 3

SEPTEMBER 1992

JOURNAL OF FOOD PROCESS ENGINEERING

All articles for publication and inquiries regarding publication should be sent to DR. D.R. HELDMAN, COEDITOR, *Journal of Food Process Engineering,* Weinberg Consulting Group Inc., 1220 19th St., N.W., Washington, D.C. 20036 USA: or DR. R.P. SINGH, COEDITOR, *Journal of Food Process Engineering,* University of California, Davis, Department of Agricultural Engineering, Davis, CA 95616 USA.

All subscriptions and inquiries regarding subscriptions should be sent to Food & Nutrition Press, Inc., 2 Corporate Drive, P.O. Box 374, Trumbull, CT 06611 USA.

One volume of four issues will be published annually. The price for Volume 15 is $120.00 which includes postage to U.S., Canada, and Mexico. Subscriptions to other countries are $139.00 per year via surface mail, and $148.00 per year via airmail.

Subscriptions for individuals for their own personal use are $100.00 for Volume 15 which includes postage to U.S., Canada, and Mexico. Personal subscriptions to other countries are $119.00 per year via surface mail, and $128.00 per year via airmail. Subscriptions for individuals should be sent direct to the publisher and marked for personal use.

The *Journal of Food Process Engineering* (ISSN: 0145-8876) is published quarterly (March, June, September and December) by Food & Nutrition Press, Inc.—Office of Publication is 2 Corporate Drive, P.O. Box 374, Trumbull, Connecticut 06611 USA. (Current issue is September 1992.)

Second class postage paid at Bridgeport, CT 06602.

POSTMASTER: Send address changes to Food & Nutrition Press, Inc., 2 Corporate Drive, P.O. Box 374, Trumbull, CT 06611.

JOURNAL OF FOOD PROCESS ENGINEERING

JOURNAL OF FOOD PROCESS ENGINEERING

Coeditors:

D.R. HELDMAN, Weinberg Consulting Group Inc., 1220 19th St., N.W., Washington, D.C.
R.P. SINGH, Agricultural Engineering Department, University of California, Davis, California.

Editorial Board:

S. BRUIN, Unilever Research Laboratory, Vlaardingen, The Netherlands
M. CHERYAN, Department of Food Science, University of Illinois, Urbana, Illinois
J.P. CLARK, Epstein Process Engineering, Inc., Chicago, Illinois
A. CLELAND, Department of Biotechnology, Massey University, Palmerston North, New Zealand
B. HALLSTROM, Food Engineering Chemical Center, S-221 Lund, Sweden
K.H. HSU, RJR Nabisco, Inc., E. Hanover, New Jersey
M. KAREL, Department of Food Science, Rutgers, The State University, Cook College, New Brunswick, New Jersey
J.L. KOKINI, Department of Food Science, Rutgers University, New Brunswick, New Jersey
J. KROCHTA, Agricultural Engineering Department, University of California, Davis, California
R.G. MORGAN, Kentucky Fried Chicken Corp., Louisville, Kentucky
S. MULVANEY, Department of Food Science, Cornell University, Ithaca, New York
T.L. OHLSSON, The Swedish Institute for Food Research, Goteborg, Sweden
M.A. RAO, Department of Food Science and Technology, Institute for Food Science, New York State Agricultural Experiment Station, Geneva, New York
S.S.H. RIZVI, Department of Food Science, Cornell University, Ithaca, New York
E. ROTSTEIN, The Pillsbury Co., Minneapolis, Minnesota
S.K. SASTRY, Department of Agricultural Engineering, Ohio State University, Columbus, Ohio
W.E.L. SPIESS, Bundesforschungsanstalt fuer Ernaehrung, Karlsruhe, Germany
J.F. STEFFE, Department of Agricultural Engineering, Michigan State University, East Lansing, Michigan
K.R. SWARTZEL, Department of Food Science, North Carolina State University, Raleigh, North Carolina
A.A. TEIXEIRA, Agricultural Engineering Department, University of Florida, Gainesville, Florida
G.R. THORPE, CSIRO Australia, Highett, Victoria 3190, Australia

Journal of
FOOD PROCESS ENGINEERING

VOLUME 15
NUMBER 3

FOOD & NUTRITION PRESS, INC.
TRUMBULL, CONNECTICUT 06611 USA

Food & Nutrition Press, Inc.
Trumbull, Connecticut USA

ISSN 0145-8876

Printed in the United States of America

CONTENTS

EFFECTS OF HIGH-PRESSURE APPLICATION ON SUBSEQUENT ATMOSPHERIC SOAKING OF CORN

SUNDARAM GUNASEKARAN

Department of Agricultural Engineering
University of Wisconsin-Madison
460 Henry Mall
Madison, WI 53706

Accepted for Publication September 26, 1990

ABSTRACT

Atmospheric-soaking tests were performed on two varieties of corn samples subjected to a pretreatment of high-pressure soaking at 10.5, 21, and 35 MPa. Soaking tests were also conducted with samples without any pretreatment at different soaking temperatures of 20, 40, 60, and 100C. Increased duration of initial high-pressure soaking was found to reduce the rate of moisture absorption during the subsequent atmospheric soaking. Predicted soaking times required for the samples to reach 45% moisture content increased with increase in applied pressure and with increase in the duration of high-pressure application. Therefore, initial high-pressure application should be limited to a low pressure level and only for a short duration. Compared with the results of the high-temperature soaking tests, initial high-pressure application does help to shorten the steeping time required at atmospheric conditions but not to the extent to compensate for the effect of high temperatures.

INTRODUCTION

Steeping of corn kernels is an important first step in the wet milling process. At this step, the kernels are soaked in warm water until the kernel moisture content reaches about 45% to facilitate easy separation of kernel components. This is a very time consuming process taking as long as 40–50 h. Long steeping periods adversely affect both kernel component recovery and production rate. In the past several years many have investigated the possibility of reducing the steeping time for wet milling. Some notable attempts include high-temperature soaking (Cox

Journal of Food Process Engineering **15** (1992) 159–167. *All Rights Reserved.*

et al. 1944; Fan *et al.* 1962; Hsu *et al.* 1983); short steeping periods interspersed between long air-rest periods (Palmer and Bathgate 1976); scarification of pericarp (Palmer 1974); and degerminating between two steeping periods (Krochta *et al.* 1981). Recently, application of high pressure has been investigated as a potential method to shorten the steeping time (Gunasekaran and Farkas 1988; Meuser *et al.* 1989). Gunasekaran and Farkas (1988) reported that application of high pressure at room temperature dramatically increased the initial imbibition of water in the kernal compared to soaking at atmospheric pressure. However, the hydration rates were found to decrease with increase in duration of high pressure application. Moreover, prolonged high pressure application will not be economically justifiable. A possible alternative is to combine both high-pressure and atmospheric soaking to take advantage of both methods. This paper presents the results of soaking tests conducted at atmospheric pressure following initial high-pressure soaking. The specific objectives were to determine the effect of high-pressure application in conjunction with subsequent atmospheric soaking at room temperature and to compare the results with that of high-temperature soaking at atmospheric pressure.

MATERIALS AND METHODS

Two varieties of corn, FRB27 × Mo17 and FRB27 × Va22, were used in this investigation. Initial moisture content of the corn was about 27%.[1] The corn samples were dried to a final moisture content of about 15% using air at 20C and 65C circulating at a rate of 2.0 $m^3/min/m^3$. Additional information on drying tests have been reported in Gunasekaran and Paulsen (1985). The samples were held in cold storage (4C, 58% relative humidity) until used for experiments. Before the soaking tests, the samples were allowed to equilibrate to room conditions. Initial moisture content of all samples were determined to be 11.2% by the oven method specified in the ASAE Standard S352.2 (ASAE 1992).

All high-pressure soaking tests were conducted using an Autoclave Engineers Isostatic Pressure Unit (Model No. IP-2-22-60) at room temperature (20C). Three pressure levels of 10.5, 21, and 35 MPa were used each for durations of 5, 10, 15 and 30 min. Three 25-g samples were used at each set of soaking conditions. The samples were taken in a 5-cm diameter polyethylene tube filled with tap water. The ends of the sample tubes were sealed using a heavy-duty stapler. These sample tubes were placed in the pressure chamber of the high pressure unit. Further details of the high-pressure soaking procedure can be found in Gunasekaran and Farkas (1988).

---

[1] All moisture contents reported are on wet basis.

After the specified duration of high-pressure application, the moisture absorbed was determined by weighing the samples. Subsequently, the samples were soaked at room temperature for about 8 h. Additional tests were conducted by soaking triplicate of 25-g samples at 20C (room temperature), 40, 60, and 100C. High-temperature soaking tests were conducted in a laboratory oven set at the desired temperatures. During these soaking tests, the samples were periodically weighed to determine the amount of moisture absorbed. Before each weighing, the samples were surface blotted with paper towel to remove the surface moisture.

RESULTS AND DISCUSSION

Moisture content of the samples after the high-pressure application are presented in Table 1. These were the initial moisture contents of the samples during the subsequent atmospheric soaking. In all atmospheric-soaking tests, the moisture absorbed varied nonlinearly with the soaking time exhibiting a power-law relationship.

TABLE 1.
MOISTURE CONTENT (%) OF CORN SAMPLES AT THE END OF HIGH-PRESSURE SOAKING

Pressure (MPa)	Soak time (min)	Drying air temperature (C)			
		20	65	20	65
		Corn: FRB27 x Mo17		Corn: FRB27 x Va22	
10.5	5	21.28	21.55	19.76	23.97
	10	21.46	23.18	20.14	24.23
	15	21.92	22.56	20.71	24.57
	30	22.92	23.80	21.83	26.08
21.0	5	19.57	20.62	19.86	23.54
	10	20.05	21.18	20.14	24.32
	15	20.33	21.64	20.43	25.00
	30	22.18	25.00	22.29	26.17
35.0	5	20.14	22.65	18.68	22.01
	10	20.62	21.83	21.00	24.75
	15	21.18	23.00	21.28	26.08
	30	21.46	23.36	21.24	26.49

$$M = a\ t^{b}$$

Where, M = moisture content (%, wet basis)
t = soaking time (h)
a, b = power law contants

The numerical values of the power-law constants a and b were determined by regressing the experimental values of M and t. All the test results conformed to the above equation with a correlation coefficient (r) of at least 0.90. Tables 2, 3, and 4 present the a and b values obtained for atmospheric soaking tests conducted following high-pressure application of 10.5, 21, and 35 MPa, respectively. The constants a and b are, respectively, the slope and intercept of the linear logarithmic plot of moisture content versus time. Therefore, "a" value can be related to the initial moisture level; and the "b" value to the rate of moisture absorption. For all three levels of high-pressure application, the "a" values showed a general increase and the "b" values a general decrease with the increased durations of high-pressure soaking. These trends indicate two aspects of the increased duration of high-pressure soaking. First, there is a slight increase in the initial grain moisture content. Second, there is a reduction in the rate of moisture absorption during the subsequent atmospheric soaking.

Similar a and b values obtained for soaking only at atmospheric pressure and at different temperature results both in increased moisture content (at any given

TABLE 2.
THE POWER-LAW CONSTANTS (a AND b) FOR PREDICTING MOISTURE CONTENT DURING SOAKING AT ATMOSPHERIC PRESSURE AFTER INITIAL HIGH-PRESSURE APPLICATION OF 10.5 MPa

Drying air temperature (C)	Period of high-pressure application (min)	Corn: FRB27 x Mo17		Corn: FRB27 x Va22	
		a	b	a	b
20	5	23.07	0.144	23.71	0.150
	10	23.95	0.131	25.19	0.138
	15	24.41	0.125	24.62	0.138
	30	24.41	0.125	25.93	0.113
65	5	21.29	0.194	26.53	0.113
	10	23.17	0.150	28.06	0.094
	15	24.30	0.119	25.45	0.119
	30	23.31	0.125	28.47	0.081

TABLE 3.
THE POWER-LAW CONSTANTS (a AND b) FOR PREDICTING MOISTURE CONTENT DURING SOAKING AT ATMOSPHERIC PRESSURE AFTER INITIAL-PRESSURE APPLICATION OF 21.0 MPa

Drying air temperature (C)	Period of high-pressure application (min)	Corn: FRB27 x Mo17		Corn: FRB27 x Va22	
		a	b	a	b
20	5	21.67	0.160	23.11	0.130
	10	23.57	0.118	23.33	0.134
	15	22.65	0.156	22.21	0.157
	30	25.68	0.105	24.91	0.100
65	5	23.44	0.151	27.54	0.090
	10	25.40	0.114	27.84	0.090
	15	25.45	0.120	28.47	0.093
	30	26.01	0.106	26.94	0.122

TABLE 4.
THE POWER-LAW CONSTANTS (a AND b) FOR PREDICTING MOISTURE CONTENT DURING SOAKING AT ATMOSPHERIC PRESSURE AFTER INITIAL-PRESSURE APPLICATION OF 35 MPa

Drying air temperature (C)	Period of high-pressure application (min)	Corn: FRB27 x Mo17		Corn: FRB27 x Va22	
		a	b	a	b
20	5	22.38	0.150	21.76	0.157
	10	24.15	0.120	23.80	0.132
	15	23.67	0.133	23.65	0.136
	30	23.09	0.135	23.53	0.127
65	5	25.64	0.124	25.02	0.145
	10	25.88	0.103	28.47	0.091
	15	25.55	0.121	28.52	0.089
	30	25.55	0.126	28.32	0.090

TABLE 5.
THE POWER-LAW CONSTANTS (a AND b) FOR PREDICTING MOISTURE CONTENT DURING SOAKING AT ATMOSPHERIC PRESSURE

Drying air temperature (C)	Period of high-pressure application (min)	Corn: FRB27 x Mo17		Corn: FRB27 x Va22	
		a	b	a	b
	20	16.60	0.200	16.01	0.181
20	40	19.93	0.213	18.51	0.228
	60	21.04	0.280	21.28	0.295
	100	23.94	0.295	25.48	0.228
	20	15.85	0.238	18.28	0.206
65	40	20.39	0.212	22.51	0.194
	60	22.13	0.273	26.20	0.210
	100	25.64	0.264	27.01	0.250

time) and in increased rate of moisture absorption. Comparing the "b" values from Tables 2, 3 and 4 with those corresponding to 20C (room temperature) in Table 5, it is clear that the rate of moisture absorption is much higher for atmospheric soaking alone than when the atmospheric soaking was preceded with high-pressure application. This is probably due to the fact that initial moisture contents for atmospheric-soaking tests preceded with high-pressure application were very high (Table 1). It is known that high-moisture samples do not absorb moisture as rapidly as low-moisture samples. All the trends were similar for both the varieties of corn and for samples dried at both drying air temperatures.

Because of the obvious differences in both a and b values, it is hard to determine the overall effect of the initial high pressure application on the moisture absorption characteristics of the samples. To have an equivalent measure of effectiveness of different treatments, total time required for the samples to reach a moisture content of 45% was calculated for each set of soaking conditions using the model parameters (Tables 6 and 7). The moisture content value of 45% was chosen to represent the approximate maximum moisture level desired in practical wet milling operation.

Table 6 shows that the predicted total soaking times required at atmospheric pressure after initial application of high-pressure vary widely. However, carefully examining the general trend it is evident that in most cases the total time required increased both with increase in the applied pressure and with increase in the dura-

TABLE 6.
PREDICTED SOAKING TIME (h) REQUIRED AT ATMOSPHERIC PRESSURE AFTER INITIAL APPLICATION OF HIGH PRESSURE TO REACH A MOISTURE CONTENT OF 45% FOR CORN KERNELS.

Drying air temperature (C)	Applied pressure (MPa)	Duration of high-pressure soaking (min)							
		Corn: FRB27 x Mo17				Corn: FRB27 x Va22			
		5	10	15	30	5	10	15	30
20	10.5	103.5	123.3	133.8	134.1	71.7	67.1	79.4	131.8
	21.0	95.5	241.2	81.8	210.6	169.8	135.8	90.3	362.0
	35.0	105.0	179.0	127.8	139.6	101.2	126.2	112.8	166.1
65	10.5	47.5	83.6	177.5	193.5	107.4	152.2	120.7	285.4
	21.0	75.87	152.4	117.2	176.7	239.9	209.0	140.6	167.8
	35.0	92.08	220.9	108.6	88.6	57.5	152.4	168.3	177.2

TABLE 7.
PREDICTED SOAKING TIME (h) REQUIRED AT ATMOSPHERIC PRESSURE FOR CORN KERNELS TO REACH A MOISTURE CONTENT OF 45%.

Soaking temperature (C)	Drying air temperature (C)			
	Corn: FRB27 x Mo17		Corn: FRB27 x Va22	
	20	65	20	65
20	146.5	80.2	301.9	79.4
40	45.8	41.9	49.2	35.5
60	15.1	13.5	12.7	13.1
100	8.5	8.4	12.1	7.7

tion of high-pressure soaking. Therefore, for best results the high-pressure application should be limited to a low pressure level and only for a short duration. As presented in Table 7, the predicted soaking times required at high temperatures are very small. Therefore, high-temperature soaking should be preferred to high-pressure application followed by soaking at atmospheric conditions. However, comparing the soaking times required at room temperature, soaking at atmospheric pressure only generally took much longer than when preceded by the brief high-pressure soaking. This indicates that the initial high-pressure application at atmospheric pressure does have its merit in shortening the steeping time but not to the extent to compensate for the effect of high-temperature soaking. Initial high-pressure application may prove to be more beneficial if carried out at above atmospheric temperatures and/or followed by above atmospheric-temperature soaking.

CONCLUSIONS

1. Increased duration of high-pressure soaking tends to reduce the rate of moisture absorption during the subsequent atmospheric soaking.
2. High-temperature soaking at atmospheric pressure is more rapid than soaking initially at a high pressure and followed by soaking at atmospheric conditions.
3. High-pressure application would help to shorten the steeping time if limited to a low pressure level and for a short duration when used as a pretreatment for soaking at atmospheric conditions.

REFERENCES

ASAE. 1992. Standard: ASAE S352.2 Moisture Measurement — Grains and Seeds. ASAE Standards, p. 404, ASAE, St. Joseph, MI 49085.

COX, M.J., MacMASTERS, M.M. and HILBERT, G.E. 1944. Effect of the sulfurous acid steep in corn wet milling. Cereal Chem. *21*, 447.

FAN, L.T., CHU, P.S. and SHELLENBERGER, J.A. 1962. Volume increase of kernels of corn and sorghum accompanying absorption of liquid water. Biotechnol. Bioeng. *4*, 311.

GUNASEKARAN, S. and FARKAS, D.F. 1988. High-pressure hydration of corn. Trans. ASAE *31*(5), 1589–1593.

GUNASEKARAN, S. and PAULSEN, M.R. 1985. Breakage resistance of corn as a function of drying rates. Trans. ASAE *28*(6), 2071–2076.

HSU, K.H, KIM, C.J. and WILSON, L.A. 1983. Factors affecting water uptake of soybeans during soaking. Cereal Chem. *60*, 208.

KROCHTA, J.M., LOOK, K.T. and WONG, L.G. 1981. Modification of corn wet-milling steeping conditions to reduce energy consumption. J. Food Processing Preservation *5*, 39.

MEUSER, F., WITTIG, J. and HUSTER, H . 1989. Effects of high-pressure disintegration of steeped maize grits on the release of starch granules from the protein matrix. Starch *41*(6), 225–232.

PALMER, G.H. 1974. Abrasion and acidulation processes in malting. Brew. Digest *49*, 40.

PALMER, G.H. and BATHGATE, G.N. 1976. Malting and brewing. In *Advances in Cereal Science and Technology, Vol. I*, (Y. Pomeranz, ed.) pp. 237–324, American Association of Cereal Chemists, Inc., St. Paul, MN.

THE FLUID MECHANICS OF COOKIE DOUGH EXTRUDERS

LEON LEVINE and ED BOEHMER

Leon Levine & Associates, Inc.,
Plymouth, Minnesota

Accepted for Publication March 18, 1992

ABSTRACT

A model of the fluid mechanics of two roll cookie dough extruders, such as used for wire cut and rout cookies, is presented. The model uses the lubrication approximation to obtain a first estimate for the predictive equations for extruder capacity, power consumption, total shear strain, and forces developed by the rolls. These equations are used to understand the importance of various design and operational parameters.

INTRODUCTION

Many cookie doughs are formed by an extrusion process which uses two counter-rotating rolls as the drivers for dough motion. If individual pieces of dough are cut as the dough extrudes from the die, this is known as a wire cut machine. This type of machine is schematically represented in Fig. 1. If a continuous ribbon of dough is formed, without cutting, this is known as a rout press (Manley 1983). This type of machine is very old. A similar machine is described in the literature (Schenkel 1966) as being used, as early as 1879, for the formation of sheets and fibers from plasticized material.

More detailed descriptions of this machinery may be found in several sources (Manley 1983; Matz 1968; Pyler 1988; Hoseney 1986). Discussion of the rheology of the doughs used for these products may be found in (Menjivar 1990; Faridi 1990).

The authors have been unable to identify any quantitative discussion of the fluid mechanics that describes these devices. The problem is clearly related to the fluid mechanics of plastic/rubber calendars and dough sheeters, which is discussed in several places in the literature (Bergen and Scott 1951; Middleman 1977; Tadmor and Gogos 1979; Levine 1985; Drew *et al.* 1987, 1988; Levine and Drew

Journal of Food Process Engineering **15** (1992) 169–186. *All Rights Reserved.*

1990, 1991). These earlier derivations will be used as a starting point for the analysis that follows.

There is some discussion of the operational performance of these machines (Manley 1983). It is pointed out that the performance of these devices is dependent on roll speed, the rheology of the dough, and the height of material in the hopper above the rolls. The plastics literature indicates (Schenkel 1966) that the production rate of these machines may be optimized by adjustment of the gap between the rolls. The optimum gap setting is indicated to be a function of the resistance of the die at the end of the extruder. This behavior is similar to that of screw extruders. It has also been observed that the rate of extrusion, and hence the weight of the finished piece, varies across the width of the rolls. The goal of this paper is to develop an approximate model that explains these observations and will allow the drawing of additional inferences about machine design and performance.

RHEOLOGY OF THE DOUGH

Figure 2 (Menjivar 1990) provides some rheological information for "typical" cookie doughs. The data for the various doughs may be described by the power law model given in Eq. (1).

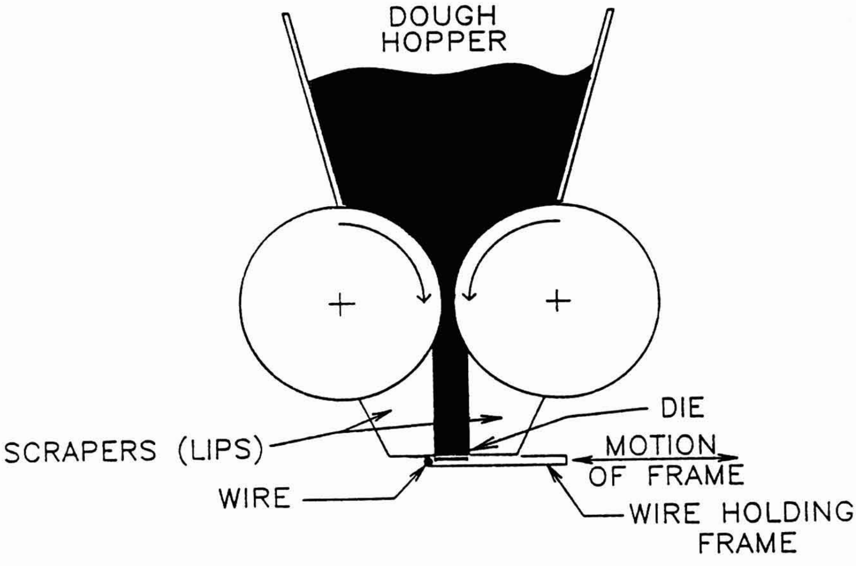

FIG. 1. SCHEMATIC REPRESENTATION OF A COOKIE DOUGH EXTRUDER

$$\tau_{xy} = K \left| \frac{\partial u_x}{\partial y} \right|^{n-1} \frac{\partial u_x}{\partial y} \tag{1}$$

For the wire cut dough, the flow consistency and flow index may be estimated as,

$$K = 3{,}650 \text{ Pa-Sec}^{0.42}$$

$$n = 0.42$$

We will develop the equations describing the fluid mechanics of the extruder using the power law model of viscosity.

MODEL DEVELOPMENT

Unlike sheeters or calendars the discharge from the rolls of cookie extruders is not "free." That is, a finite pressure exists at the point where the dough leaves the rolls and enters the "lips." Since these lips also function as doctor blades, the resistance that the lips present to flow is a function of their length, positioning and roll gap. The combination of positioning and roll gap define the spacing of the slot formed by the lips. As a consequence, the model must simultaneously consider the fluid mechanics associated with the rolls and the lips.

Fortunately, the equations for the flow between wide rolls are described in the literature (Middleman 1977). These equations assume that the lubrication approx-

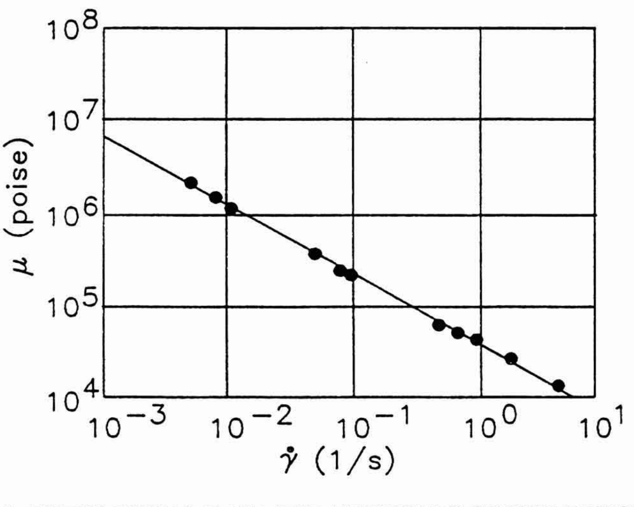

FIG. 2. RHEOLOGICAL DATA FOR "TYPICAL" COOKIE DOUGH (MENJIVAR 1990 WITH PERMISSION)

imation is valid. That is, the solutions neglect inertial effects and assume that the flows in the direction of pumping are much greater than the flows in the direction normal to the rolls. Under these conditions the Navier-Stokes equation reduces to,

$$0 = -\frac{dp}{dx} + \frac{\partial}{\partial y}\tau_{xy} \tag{2}$$

The literature (Middleman 1977; Tadmor and Gogos 1979; Tanner 1985) discusses some of the implications associated with applying the lubrication approximation to this problem. The approximation neglects viscoelastic effects, extensional flow phenomenon, and the circulatory flows that may develop at the inlet to the rolls. None the less, the results obtained by using the lubrication approximation have been shown to, at least, qualitatively describe the pressure developed between roll. The effect of the lubrication approximations would be to underestimate the forces acting on the rolls and the power required to turn the rolls.

The geometry used to develop the equations is described by Fig. 3. The literature (Middleman 1977) provides the dimensionless pressure gradient developed between the rolls. This is provided in Eq. (3).

$$\frac{dp'}{dx'} = -\left(\frac{2n+1}{n}\right)^n \sqrt{\frac{2R}{H_0}}\,\frac{(\lambda^2 - x'^2)\,|\lambda^2 - x'^2|^{n-1}}{(1 + x'^2)^{2n+1}} \tag{3}$$

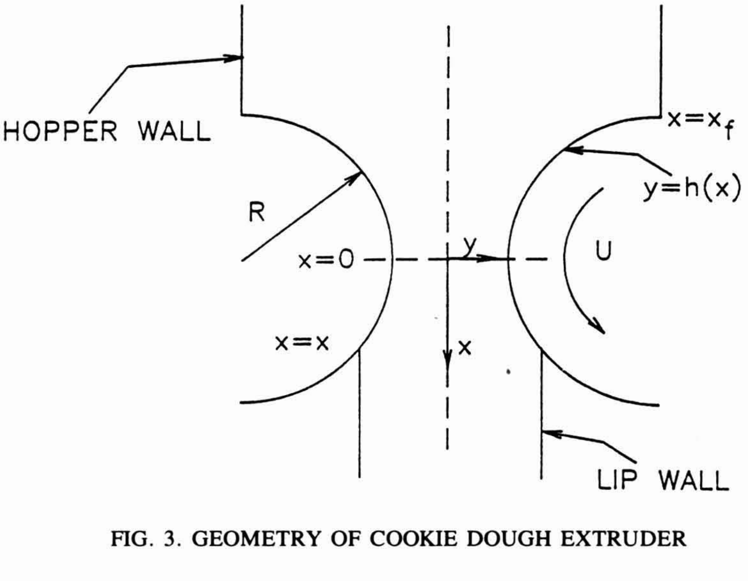

FIG. 3. GEOMETRY OF COOKIE DOUGH EXTRUDER

The parameter, λ, is a dimensionless roll output per unit width. It is defined by,

$$\lambda^2 = \frac{Q}{2UH_0} - 1 \tag{4}$$

The dimensionless position and pressure, x′ and p′, are defined by,

$$x' = \frac{x}{\sqrt{2RH_0}} \tag{5}$$

$$p' = \frac{p}{K}\left(\frac{H_o}{U}\right)^n \tag{6}$$

The velocity profile between rolls is defined by,

$$u_x = U + \frac{1}{q}\left(\frac{1}{K}\frac{dp}{dx}\right)^{1/n}[y^q - h^q(x)] \tag{7a}$$

$$u_x = U - \frac{1}{q}\left(-\frac{1}{K}\frac{dp}{dx}\right)^{1/n}[y^q - h^q(x)] \tag{7b}$$

Equation (7a) applies when the pressure gradient is positive, and Eq. (7b) applies when the pressure gradient is negative.

The pressure as function of position may be obtained by integration of Eq. 3. In dimensionless form,

$$p' - p'_o = \left(\frac{2n+1}{n}\right)^n \sqrt{\frac{2R}{H_0}} \int_{-x'_f}^{x'} \frac{|\lambda^2 - x'^2|^{n-1}(x'^2 - \lambda^2)}{(1 + x'^2)^{2n+1}}\, dx' \tag{8}$$

The lower boundary of the integration is not zero to allow for the presence of a head at the feed of the rolls as a result of high levels of fill in the hopper.

It is assumed that the lips form a channel whose sides are parallel to one another and that the rolls are very wide. This allows the lips to be considered as a simple slot. The equations for the flow of a power law fluid through a wide slot is given by (Schenkel 1966),

$$Q = \frac{n(2H)^2}{2(2n+1)}\left[\frac{HP_{\text{lips}}}{LK}\right]^{1/n} \tag{9}$$

The total pressure developed at the discharge of the combined system, ignoring entrance effects at the lip feed, is the difference between the pressure developed at the discharge of the rolls and the pressure fall through the lips. (Entry effects may be considered by replacing the lip length in Eq. 9, with a longer effective length.) The pressure developed is available for pushing product through the die.

Figure 4 illustrates the pressures and pressure changes that are developed within the system. The net pressure rise developed by the system is the difference between the pressure rise developed by the rolls and the pressure drop in the lips.

$$P_{rise} = p - P_0 - P_{lips} \tag{10}$$

Again referring to Fig. 4, the pressure available to push the dough through the die (the die pressure drop) is given by Eq. 11.

$$P_{die} = P_{rise} + P_0 \tag{11}$$

Recognizing the output of the extruder and the output of the die are identical, the actual operating condition of the extruder is determined by the intersection of the extruder output curve and the die output curve. This is illustrated in Fig. 5. This view makes it obvious that the performance of the extruder is directly tied to the particular die used to form the cookie shape.

The problem is now solved by choosing a dimensionless output and integrating Eq. (10). Before this is done, some "typical" values (Kuipers 1991) for the lip length, and lip and hopper position must be chosen. Table 1 summarizes the values

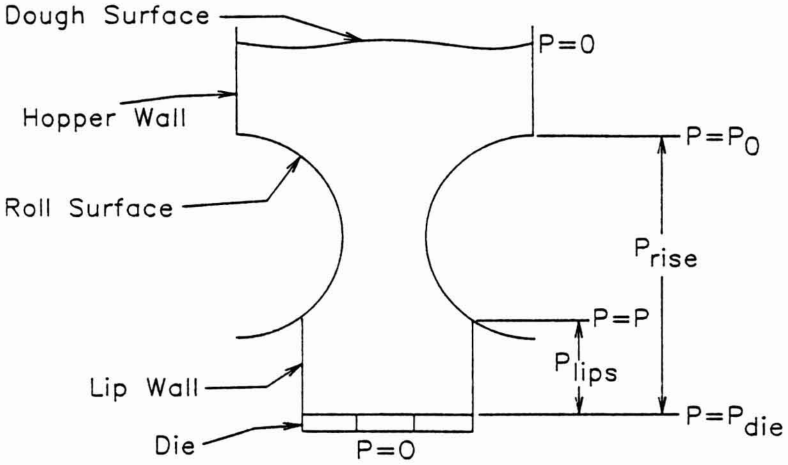

FIG. 4. PRESSURES AND PRESSURE CHANGES DEVELOPED IN SYSTEM

TABLE 1.
TYPICAL EXTRUDER GEOMETRY

Item	Value (in roll Radii)
Distance of hopper from nip	1.0
Distance of lips from nip	0.5
Length of lips	1.0

used for the calculation. The integration has been accomplished through the use of a commercially available mathematics program, MathCAD™ (MathSoft, Inc., Cambridge Mass.) The program uses Simpson's rule to perform numerical integrations. The convergence accuracy of the integration was specified to be not less than 1%.

The results of these integrations, for three different flow indices, are presented in Figures 6, 7 and 8 as plots of dimensionless output versus dimensionless discharge pressure, with dimensionless gap as a parameter.

Figures 6, 7, and 8 are analogous to the operating curves for the two-plate model of extruders that is widely discussed in the literature (Middleman 1977; Harper 1981; Levine 1988). One conclusion can immediately be drawn in this case: the roll radius is somewhat analogous to length of the extrusion screw. The larger radius results in the ability to develop higher discharge pressures or more capacity at the same discharge pressure. In addition, the effect of hopper fill level is readily apparent. Deep hoppers create a head at the contact point with the rolls. This results in a higher pressure delivered to the die per Eq. (11) and hence a direct increase in the output for a particular resistance curve. The significance of this effect is a function of the rheology of the dough, the operating conditions of the extruder, and the resistance of the die assembly.

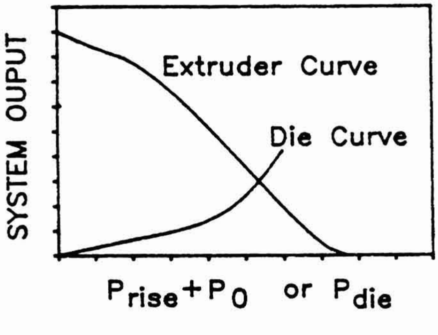

FIG. 5. INTERACTION OF EXTRUDER AND DIE

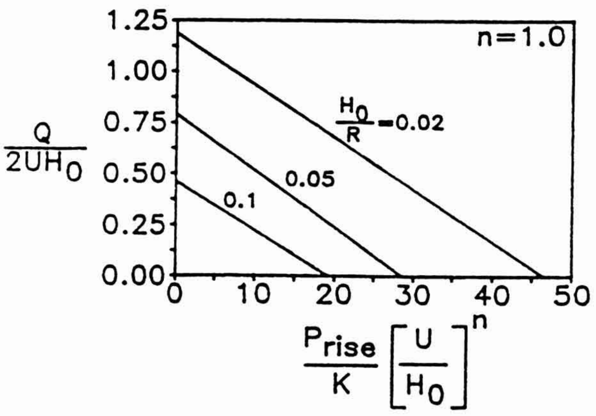

FIG. 6. DIMENSIONLESS OUTPUT VERSUS DIMENSIONLESS PRESSURE RISE: FLOW INDEX 1.0

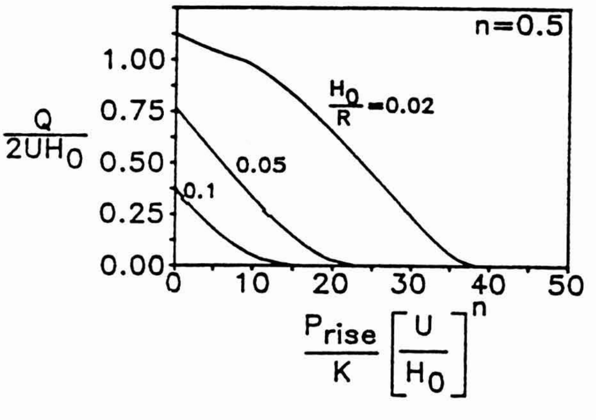

FIG. 7. DIMENSIONLESS OUTPUT VERSUS DIMENSIONLESS PRESSURE RISE; FLOW INDEX 0.5

The analogy between roll radius and screw length can be improved by considering a change in the position of the feed hopper. As the feed hopper is moved closer to the nip, the "screw" becomes shorter and the pressure development capability of the "screw" becomes significantly less. This is illustrated for one gap and flow index in Fig. 9. Note that reducing the fill level of the hopper below the hopper's contact point with the roll is identical to moving the hopper closer to the nip, so this is one additional explanation for the importance of controlling hopper level.

Because the gap between the rolls appears in both the ordinates and abscissas of Fig. 6, 7, and 8 the effect of this variable is not readily apparent. Figure 10

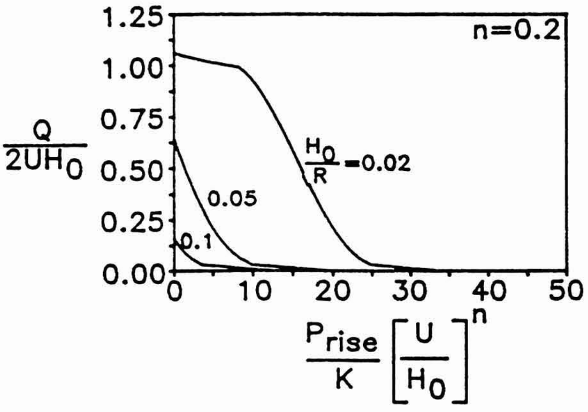

FIG. 8. DIMENSIONLESS OUTPUT VERSUS DIMENSIONLESS PRESSURE RISE; FLOW INDEX 0.2

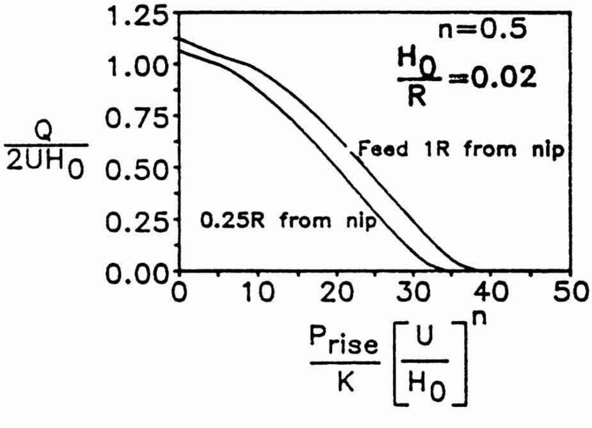

FIG. 9. EFFECT OF HOPPER POSITION ON OUTPUT

is a replot of the data in Fig. 7. In this case the gap has been removed from the definitions of the axis. Figure 10 reveals, as suggested by the literature (Schenkel 1966) that, analogous to the thread depth of single screw extruders, there is a roll gap setting that optimizes the output of the rolls. The optimum gap setting is directly related to the resistance of the die assembly. For example, for a low resistance die (a die that passes larger volumes at low pressure drops) the highest production is achieved with a large gap. At intermediate die resistances the maximum output may be achieved with an intermediate gap, and with the highest die resistances the highest output is obtained with a small roll gap.

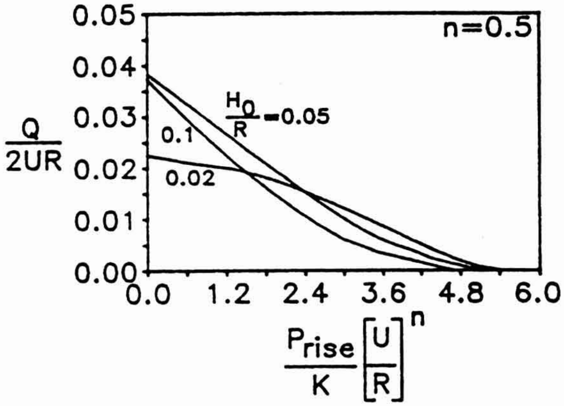

FIG. 10. ILLUSTRATION OF OPTIMUM GAP

Integration of the pressure profile across the face of the rolls provides us with another additional useful piece of engineering information, the force exerted on the dough by the rolls. This information is needed in order to mechanically specify the bearing and shafts, and to estimate how much deflection of the roll results in wider gaps at the center than at the edges. This causes increased flow rates at the center of the roll. This is reflected in final cookie size or mass and is one observed explanation for weight variation across the width of the roll.

The force per unit width is given by,

$$F = \int_{-x_f}^{x_o} p\, dx \tag{12}$$

This integration has been carried out numerically. The results are presented in Fig. 11, 12 and 13 as dimensionless force versus dimensionless discharge pressure with dimensionless gap as a parameter. Higher speeds, and at fixed roll speeds, smaller gaps, higher pressure, and larger roll diameters result in greater forces on the rolls.

Another value that would be useful for the model to calculate is the work input of the rolls. This is needed in order to accomplish the task of sizing the motor required to drive the device. In addition, work input is often indicated as a cause of the effect of the processing device on the quality of the dough. The power transmitted to the rolls per unit width is given by,

$$P_{ow} = 2 \int_{-x_f}^{x_o} \tau_{xy} \Big|_{y=h(x)} U\, dx \tag{13}$$

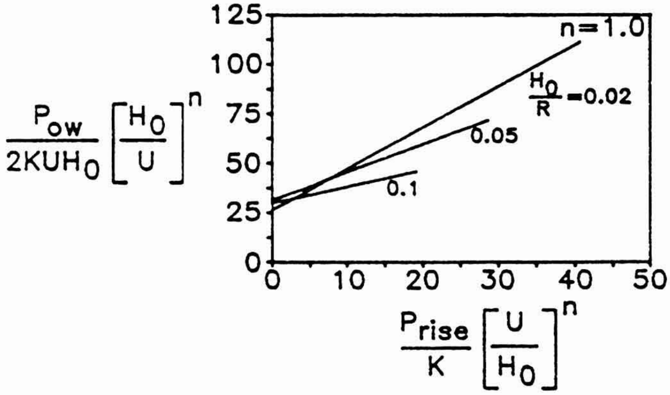

FIG. 11. DIMENSIONLESS POWER CONSUMPTION VERSUS DIMENSIONLESS PRESSURE RISE; FLOW INDEX 1.0

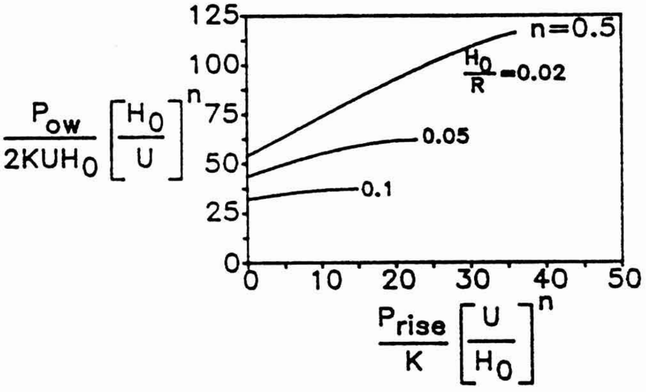

FIG. 12. DIMENSIONLESS POWER CONSUMPTION VERSUS DIMENSIONLESS PRESSURE RISE; FLOW INDEX 0.5

The shear stress is obtained through the use of the pressure profile and the velocity profiles (Eq. 3, 7a, b). The velocity profiles are differentiated to obtain the local shear rate, and Eq. (1) is used to obtain the local shear stress. The integration indicated by Eq. (13) is then carried out.

As before, the results of the integration of Eq. 13 is presented in dimensionless form in Fig. 14, 15, and 16. Higher speeds, and at fixed roll speeds, smaller gaps, higher pressure, and larger roll diameters result in greater power consumption in turning the rolls.

The work input per unit throughput of the system is now calculated by combining the results of Fig. 6, 7, or 8 with the appropriate power curve of Fig.

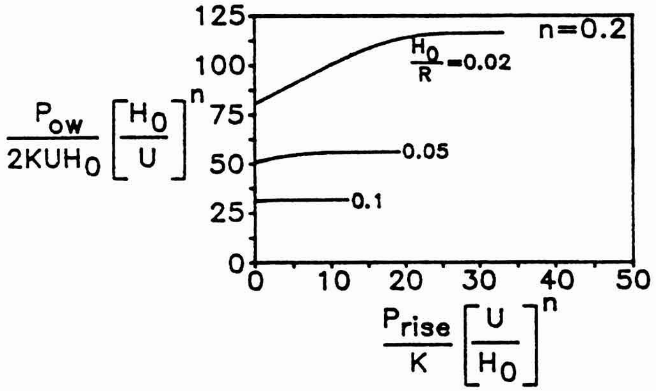

FIG. 13. DIMENSIONLESS POWER CONSUMPTION VERSUS DIMENSIONLESS PRESSURE RISE; FLOW INDEX 0.2

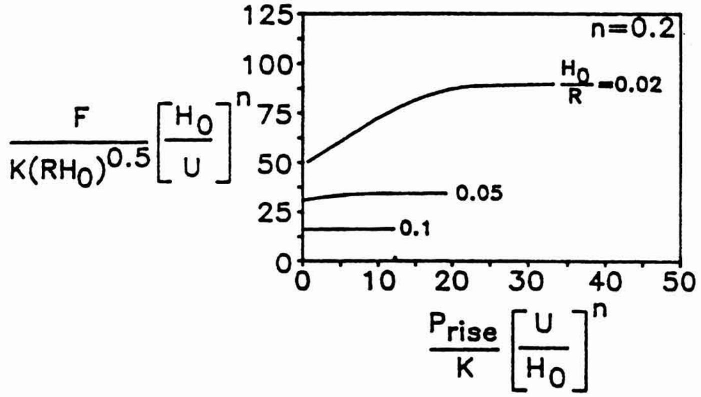

FIG. 14. DIMENSIONLESS FORCE VERSUS DIMENSIONLESS PRESSURE RISE; FLOW INDEX 1.0

14, 15, or 16. An example result is presented in Fig. 17. The work input per pound increases with roll radius. This is the price that is paid for designing stiffer, larger diameter rolls. The curve also indicates that at lower die output resistances a gap may exist that minimizes work input, this is somewhat similar to the performance of screw extruders.

There is one final item that may be of interest. It is often observed that excessive shear results in coalescence and "oiling out" of droplets of oil contained in the dough. One mechanism for this phenomenon may be similar to the coalescence that is observed in the emulsions undergoing stirring. The phenomenon

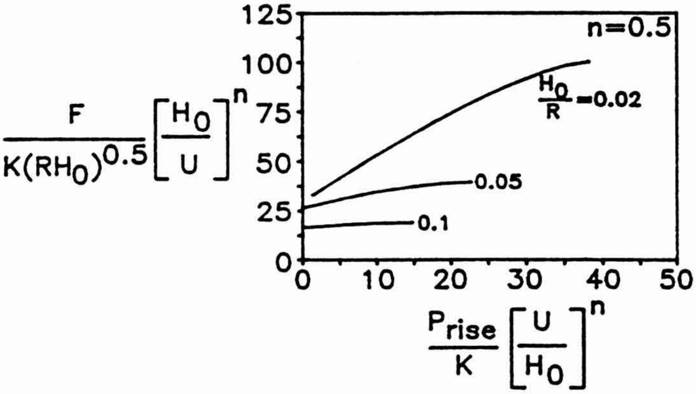

FIG. 15. DIMENSIONLESS FORCE VERSUS DIMENSIONLESS PRESSURE RISE; FLOW INDEX 0.5

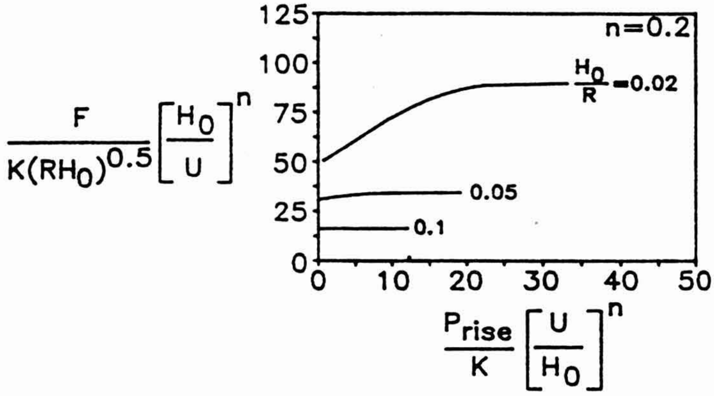

FIG. 16. DIMENSIONLESS FORCE VERSUS DIMENSIONLESS PRESSURE RISE; FLOW INDEX 0.2

is sometimes referred to as orthokinetic flocculation (Bisio and Kabel 1985). The coalescence is the result of the collision of oil droplets that reside on different flow stream lines. As the result of the velocity gradients (shear rates) within the system, some droplets are moving faster than others. Given time, droplets on fast streamlines will overtake those on slow streamlines, resulting in a collision. The number of collisions that will occur is directly related to the product of shear rate and time of exposure. This is best expressed as the weighted average total shear strain. The weighted average total shear strain, a dimensionless quantity, is defined by,

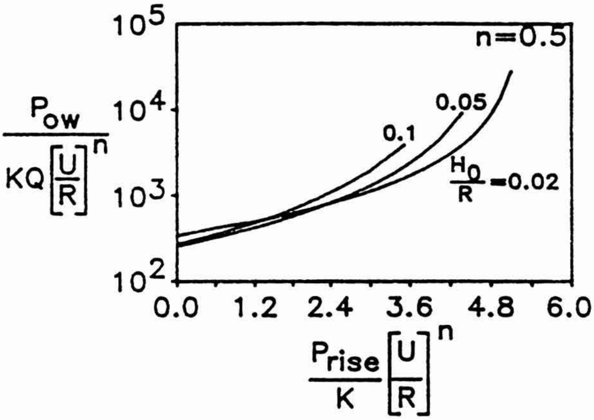

FIG. 17. EFFECT OF ROLL RADIUS ON WORK INPUT

$$\overline{\gamma} = \frac{1}{Q}\int_{-x_f}^{x}\int_{-h(x)}^{h(x)}\frac{dU_x}{dy}\,dy\,dx \tag{14}$$

Figure 18, 19, and 20 are presentations of the results of these calculations. As the roll radius and velocity increase, the gap decreases, and the pressure increases, the total shear strain increases, indicating an increased tendency for coalescence. The results indicate that at lower die output resistances a gap may exist that minimizes shear strain.

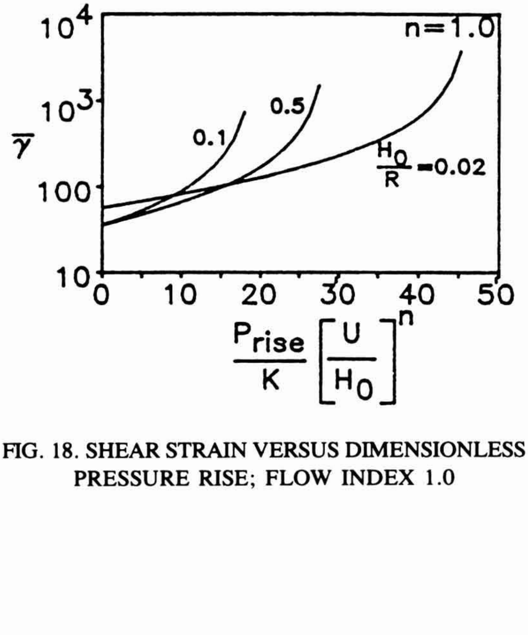

FIG. 18. SHEAR STRAIN VERSUS DIMENSIONLESS PRESSURE RISE; FLOW INDEX 1.0

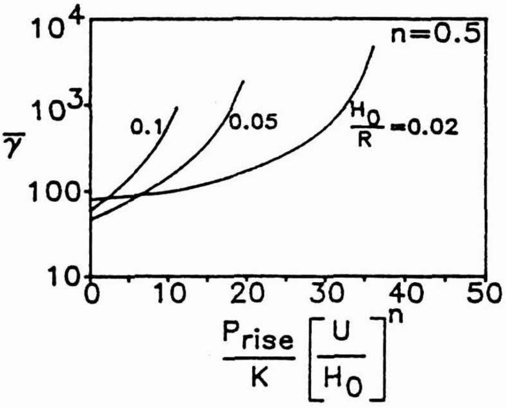

FIG. 19. SHEAR STRAIN VERSUS DIMENSIONLESS PRESSURE RISE: FLOW INDEX 0.5

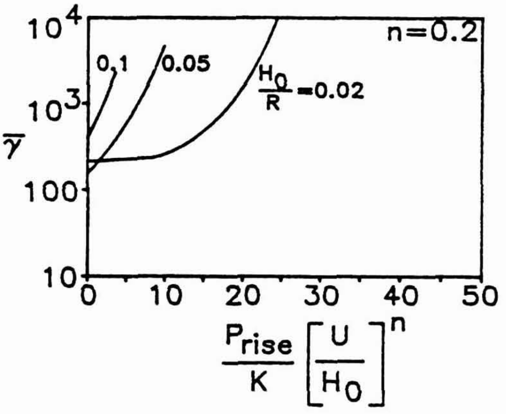

FIG. 20. SHEAR STRAIN VERSUS DIMENSIONLESS PRESSURE RISE; FLOW INDEX 0.2

CONCLUSIONS

Examination of the fluid mechanics of cookie dough extruders by this means can be extremely useful in predicting design and performance criteria. The theory indicates that the performance of these extruders is somewhat analogous to that of extrusion screws. The important machine design variables are roll radius and speed, gap setting, hopper design, and lip design. If knowledge of the rheological properties of the cookie doughs is available, the model allows one to estimate roll pumping capacity, roll forces, roll power consumption, and the total shear strain exerted on the dough, as well as the work input to the dough.

The following conclusions about extruder performance/design can be drawn from the model:

(1) For a given die resistance, the model indicates that an optimum gap exists, which maximizes extruder output.

(2) For a given power and shear strain, the model indicates that an optimum gap exists, which maximizes extruder output.

(3) As the roll radius increases, the output of the extruder increases at the cost of increased energy input to the dough and total shear strain on the dough.

(4) As the roll speed increases, the output of the extruder increases at the cost of increased energy input to the dough and total shear strain on the dough.

(5) The model indicates that narrowing the hopper or lowering the level in the hopper decreases the output of the extruder.

NOMENCLATURE

F	Closing force per unit width
H	Half the space between the lip walls
H_0	Half gap
h(x)	Distance from the center line to the roll surface at any position, x
k	Power law consistency
L	Length of lips
n	Power flow index
p	Pressure
p'	Dimensionless $= (p/K)(H_0/U)^n$
p'_0	Dimensionless pressure at the feed of the rolls
P_{die}	Die pressure drop
P_{ow}	Power consumption
P_0	Pressure at the contact point of the hopper
P_{rise}	Pressure increase between the rolls
P_{lips}	Pressure resistance of the lips
Q	Volumetric flow rate per unit roll width
q	Exponent used in Eq. (8a) and (8b) $= (1 + n)/n$
R	Roll radius
U	Roll surface velocity
u_x	Velocity in direction of flow
x	Direction of flow
x'	Dimensionless × direction $= x/\sqrt{2RH_0}$
x_f	X-coordinate of the point of contact with the hopper

x'_0	X-coordinate of point of contact with the lips
y	Direction normal to flow
γ	Shear rate
$\bar{\gamma}$	Total strain
λ	Dimensionless ouput (Eq. 6)
μ	Viscosity
τ_{xy}	Shear stress

REFERENCES

BERGEN, J.T. and SCOTT, B.W. 1951. Pressure distribution in the calendering of plastic materials. J. Appl. Mech. *18*, 101–106.

BISIO, A. and KABEL, R.L. 1985. *Scale-Up of Chemical Processes*, John Wiley & Sons, New York.

DREW, B., LEVINE, L. and RAMKRISHNA, V. 1988. Numerical solution to a problem in the flow of viscoelectric fluid between rotating cylinders. Paper read at the National Meeting of the Society for Industrial and Applied Mathematics, 13–15 July, Minneapolis, Minn.

DREW, B., LEVINE, L., RAMKRISHNA, V. and CLEMMINGS, J. 1987. Comparison of mathematical models of dough sheeted through rolls. Paper read at the National Meeting of the American Institute of Chemical Engineers, 17–19 Aug., Minneapolis, Minn.

FARIDI, H. 1990. Application of rheology in the cookie and cracker industry. In *Dough Rheology and Baked Product Texture*, (H. Faridi and J.M. Faubion, eds.) pp. 363–384, Van Nostrand Reinhold, New York.

HARPER, J.M. 1981. *Extrusion of Foods, Vol. I*, CRC Press, Boca Raton, Fla.

HOSENEY, R.C. 1986. *Principles of Cereal Science and Technology*, American Assoc. of Cereal Chemists, St. Paul, Minn.

KUIPERS, D. 1991. Personal correspondence with APV Baker Inc., Grand Rapids, Mich.

LEVINE, L. 1985. Throughput and power of dough sheeting rolls. J. Food Proc. Eng. *7*, 223–228.

LEVINE, L. 1988. Understanding extruder performance. Cereal Foods World *3*(12), 963–970.

LEVINE, L. and DREW, B.A. 1990. Rheological and engineering aspects of the sheeting and laminating of doughs. In *Dough Rheology and Baked Product Texture*, (H. Faridi and J.M. Faubion, eds.) pp. 513–556, Van Nostrand Reinhold, New York.

LEVINE, L. and DREW, B.A. 1991. Rolling and laminating of cookie and cracker doughs. In *Cookie and Cracker Technology*, (H. Faridi, ed.), Van Nostrand Reinhold, New York.

MANLEY, J.R. 1983. *Technology of Biscuits, Crackers and Cookies*, Ellis Horwood Limited, Chichester, England.

MATZ, S.A. 1968. *Cookie and Cracker Technology*, Van Nostrand Reinhold/AVI, New York.

MENJAVAR, J.A. 1990. Fundamental rheological properties of model cookie and cracker doughs. Paper read at the 75th Annual Meeting of the American Association of Cereal Chemists Abstr. No. 33.

MIDDLEMAN, S. 1977. *Fundamentals of Polymer Processing*, McGraw-Hill Book Co., New York.

PYLER, E.J. 1988. *Baking Science and Technology, Vol. II*. Sosland Pub. Co., Merriam, Kansas.

SCHENKEL, G. 1966. *Plastics Extrusion Technology and Theory*, American Elsevier Pub. Co., New York.

TADMOR, Z. and GOGOS, C.G. 1979. *Principles of Polymer Processing*, John Wiley & Sons, New York.

TANNER, R.I. 1985. *Engineering Rheology*, Clarendon Press, Oxford.

INFLUENCE OF CONCENTRATION OF MILK SOLIDS ON FREEZE-DRYING RATE OF YOGHURT AND ITS QUALITY[1]

N.K. SHARMA

Department of Mechanical Engineering
G.P. Pant University Of Agriculture and Technology
Pantnagar (Nainital)
U.P. (263145)
India

C.P. ARORA

Department of Mechanical Engineering
Indian Institute Of Technology
New-Delhi (110016)
India

and B.K. MITAL

Department Of Food Science and Technology
G.B. Pant University Of Agriculture & Technology
Pantnagar (Nainital)
U.P. (263145)
India

Accepted for Publication May 28, 1992

ABSTRACT

An increase in milk solids in yoghurt from 14.7 to 20.4%, obtained by adding NFDM (2–8% wv) to whole cow milk enhances the yield of freeze-dried yoghurt from 0.2196 to 0.3067 kg/(m².h). A reduction of 25.8% in drying time per unit output occurs when the concentration of milk solids in yoghurt increases from 14.7 to 18.8%. A further increase in the solids concentration of yoghurt from 18.8 to 20.4% results in a 5.7% reduction in the drying time. Organoleptic evaluation showed that an increase in the milk solids to 18.8% enhances the acceptability of the product. A further increase in the level of milk solids imparts a chalky taste to the product.

---

[1] Research Paper no. 6467 through the Experiment Station, G.B.P.U.A.T., Pantnagar, Nainital (U.P.).

Journal of Food Process Engineering **15** (1992) 187–198. *All Rights Reserved.*

INTRODUCTION

Yoghurt is a common ingredient of diet because of its nutritional and therapeutic value (Deeth and Tamime 1981; McDonough *et al.* 1982; Savaiano and Levitt 1984). Because of these attributes, it is not only consumed directly but efforts have also been made to incorporate it in the manufacturing of products such as yoghurt-flavored wafers, chocolates and various dietetic foods (Winwood 1987). However, the shelf-life of yoghurt in its natural form is short but can be enhanced either by spray or freeze drying. The latter method is more suitable for retaining its original biological characteristics (Vitanov *et al.* 1973).

Gavin (1968) found that plain yoghurt after freeze drying loses its original characteristics and flavor on rehydration. Vietz (1966) observed that the acetaldehyde level originally present in yoghurt is reduced by about 75% after freeze drying. Radaeva *et al.* (1970) froze yoghurt at −25C, dried it at 23–30C for 9–10 h, and found that the product has excellent keeping but poor reconstitution qualities. Blanchaud (1972) added sucrose/glucose, fruit pulp and milk powder to yoghurt and freeze dried the mixture to instant yoghurt powder. Vitanov *et al.* (1973) observed that the quality of freeze-dried Bulgarican yoghurt is considerably influenced by the strain used for fermenting the milk. Toei (1984) observed that not only the physicochemical properties of the product but also the drying method used, i.e., the contact and radiative heating influences its freeze drying rate. Little is known about the effect of freeze-drying conditions, such as the compositional characteristics of the material to be freeze dried, the freezing rate, the temperatures of freezing and drying on the product quality. Franks (1989) stated that the quality of the final product can be improved by simple changes in the formulation and/or the freezing and drying conditions.

The objective of this study was to determine the effect of milk solids in yoghurt on its freeze-drying rate and the quality of the reconstituted product.

MATERIALS AND METHODS

Materials

Fresh cow milk obtained from Livestock Research Centre of the University of Pantnagar, India, was used for this study.

Cultures

Streptococcus thermophilus-YHS and *Lactobacillus delbrueckii* subsp. *bulgaricus*-YHL obtained from National Dairy Research Institute Karnal, India were used to prepare the yoghurt. The cultures were maintained in sterilized skim milk by fortnightly transfers, and stored at 4 ± 1C between transfers.

Yoghurt Preparation

For yoghurt preparation, the milk was heated to 85C for 30 min. The total solids in milk were increased by adding nonfat dry milk (NFDM) (moisture 5%, fat 2.7%, protein 35.0%) at 2, 5, and 8% (w/v) levels. The resultant solids in the yoghurt are 14.7% without addition of NFDM, and 16.3%, 18.8% and 20.4% with the addition of NFDM. The milk was then cooled and inoculated with *S. thermophilus* and *L. delbrueckii* subsp. *bulgaricus* in the ratio of 1:1 @ 3% v/v. The inoculated milk was incubated at 42C for 3.5 h. The yoghurt thus prepared was kept at 4 ± 1C until use.

Freeze-Drying Apparatus

The drying chamber has a cylindrical stainless steel enclosure with an inside diameter of 0.23 meter and an inside depth of 0.30 meter. A transparent cover permits the visual inspection of the inside of the vacuum chamber during the freeze-drying process. The vacuum is produced using a two-stage rotary vacuum pump with a displacement of 150 L; about 5 min are required to obtain 0.52 mbar in the chamber. The vacuum was measured using a vacuscope and a Pirani gauge. The compressor maintained a temperature of −54 ± 3C in the cylindrical condenser.

Drying Method

Twenty four grams of yoghurt sample were transferred to a sample vessel and placed in a deep freezer along with platen and left overnight at −24C. Before loading the samples, the freeze dryer was run for about 2 h to obtain a constant minimum temperature of −54 ± 3C in the condenser. Samples were placed symmetrically on the circular aluminium platen (20 cm dia.) fitted with a micro-heater at the bottom. A constant minimum temperature of the sample was obtained after about 20 min. Thereafter, heater supply was switched on and the samples were dried for a specified time after which the samples were removed, weighed quickly and discarded. The process was repeated till constant weight of the sample was obtained. The temperature of the heater plate and at various locations in the samples were measured with a copper-constantan (30 gauge) thermocouple and Philips (PPX 9004) microvoltmeter. A temperature controller automatically adjusted the heater-platen temperature to 45 ± 3C. The pressure in the vacuum chamber ranged from 1.3 mbar at the beginning of the drying run to 0.52 mbar at the end of a test. After the drying process was complete, the samples were removed and stored in glass-stoppered containers at 4 ± 1C until use.

Chemical Analysis

The fat content of the milk and the freeze-dried yoghurt was measured by the Gerber method and by Soxhlet extraction, respectively (APHA 1972). The protein in a sample was determined by the Kjeldahl method using a nitrogen-to-protein conversion factor of 6.38 (AOAC 1980). Ash and moisture in the samples were calculated according to AOAC (1980) procedures. The lactic acid in reconstituted yoghurt (dried yoghurt: water = 1:3.5, w/v) was determined by titrating 10 g of the sample with 0.1 N NaOH using phenolphthalein as the indicator and computing on a dry basis (I.S.I. 1981).

Sensory Evaluation

The acceptability of the reconstituted freeze-dried yoghurt samples was determined by multi-comparison test (Larmond 1977) using freeze-dried yoghurt without added NFDM as the reference. The samples were reconstituted in water at a ratio of 1:3.5 (w/v), and cooled to 4 ± 1C before serving. The sensory panel consisted of 6 trained judges of the department of Food Science and Technology. The samples were evaluated for color, flavor and texture on a scale ranging from 1 to 9, where 1 represented extremely inferior to the reference and 9 represented extremely better than the reference. The samples were served at random to same panelists for two replications of study.

RESULTS AND DISCUSSION

In thermal contact heating of the frozen layer during freeze drying, it is essential to seal the face receiving heat supply against vapor flow. There is a tendency for drying to take place from the edges of the frozen layer and at surfaces in contact with the heating platen. Mellor (1978), has suggested drying at lower plate temperatures in metal trays or by superimposing thin plastic sheets between the bottom of the tray and the underside of the frozen layer to overcome these difficulties. Metal trays would promote growth of dry layer at the edges, since vapor generated can easily escape. Quast and Karel (1968) used a circular dish with Lucite side walls and flat brass bottom in freeze drying of coffee. They reported drying from the sides and from the bottom of the sample as a frequent source of irregularity in the drying curves. These difficulties were overcome by using a circular product tray made of nylon side walls and flat aluminium bottom (Fig. 1). To promote good contact between the product bottom and tray, steel pins fixed radially through the side walls and extending into the product were used in this study. These pins kept the product in good contact with the tray during drying and helped check the growth of the dry layer at product bottom-tray interface and product separation. During several trials, samples were removed from the drying chamber at various times and cut to see the growth of dry layer. It was observed that sample bottom-tray interface always exhibited a frozen state.

The weight loss as a function of drying time for the yoghurt samples with different total solids (14.7–20.4%) is shown in Fig. 2. After drying for 4.5 h, moisture determinations showed that the moisture loss of the samples had become negligible. Therefore, the end point of drying was taken as 4.5 h. Due to the large thermal contact resistance between the heater-platen and the product-tray interface, the temperature at the product bottom-tray interface varied from −19 to −3C during sublimation. The placement of the sample on the heater-plate, in the drying chamber influenced the drying rate. The drying rate decreased as the sample vessel was moved away from the center of the heater-platen. Therefore, the sample vessels were placed symmetrically on the heater-platen. The percentage weight loss of the different yoghurt samples after 4.5 h of drying was 78.33, 80.0, 82.5 and 84.5% for yoghurt containing 20.4, 18.8, 16.3 and 14.7% milk solids, respectively (Fig. 2).

The moisture remaining in the samples at any given time during drying decreased with the decrease in concentration of solids. The drying rate curves for the various samples are shown in Fig. 3. During the sublimation phase the drying rate exhibited a decrease with an increase in milk solids in yoghurt. In contrast, during desorption, the drying rate increased slightly with an increase in milk solids. The decrease in drying rate with an increase in concentration of milk solids during

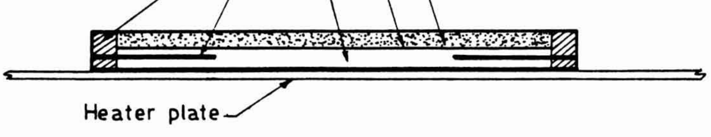

FIG. 1. SCHEMATIC OF PRODUCT TRAY

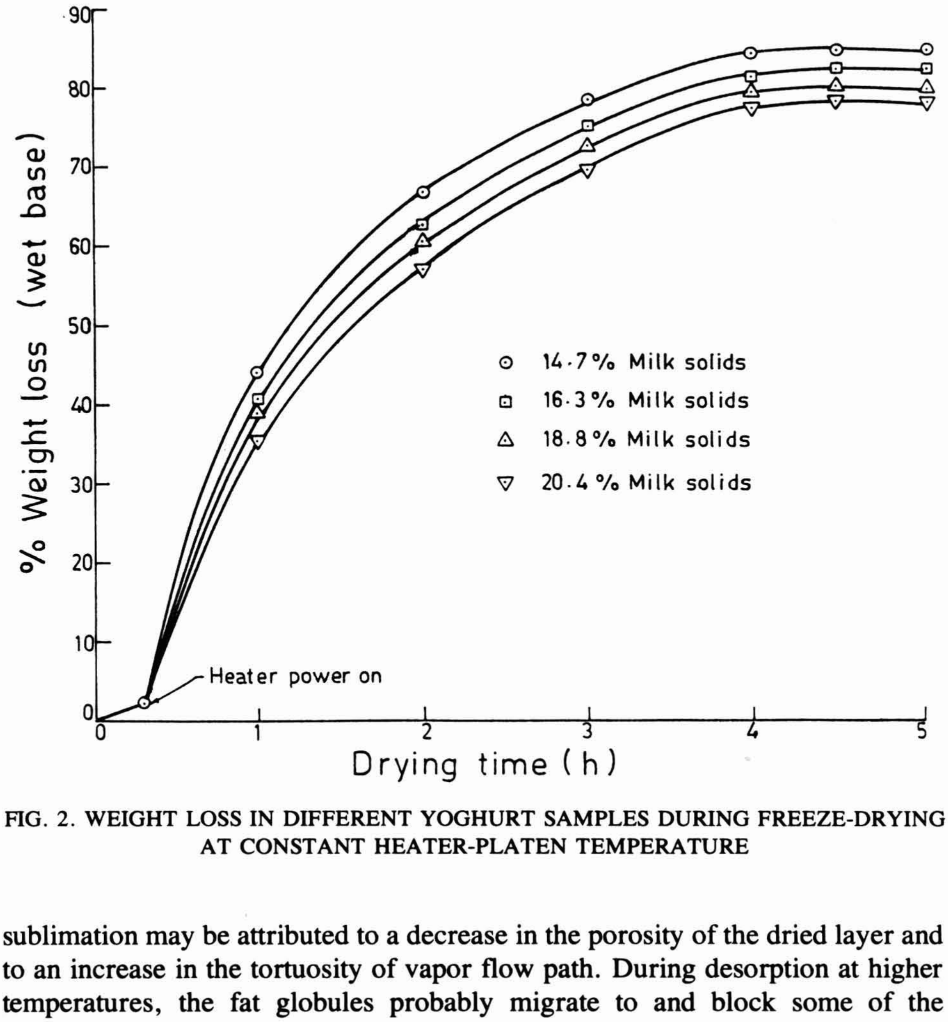

FIG. 2. WEIGHT LOSS IN DIFFERENT YOGHURT SAMPLES DURING FREEZE-DRYING AT CONSTANT HEATER-PLATEN TEMPERATURE

sublimation may be attributed to a decrease in the porosity of the dried layer and to an increase in the tortuosity of vapor flow path. During desorption at higher temperatures, the fat globules probably migrate to and block some of the capillaries, resulting in a decrease in the drying rate.

In the present investigation, nonfat dry milk was used to enhance the concentration of milk solids in the product. Consequently, the number of fat globules per unit volume of the product decreased with an increase in the level of nonfat dry milk. Therefore, the increase in the drying rate during desorption of the different samples may be attributed to the decrease in the number of blocked capillaries due to the increased level of the additive.

Kumagai *et al.* (1984) observed a constant rate period during freeze drying of milk with back-face heating. However, no constant rate period was observed in this study. The drying rate depends on the characteristics of the dry layer matrix.

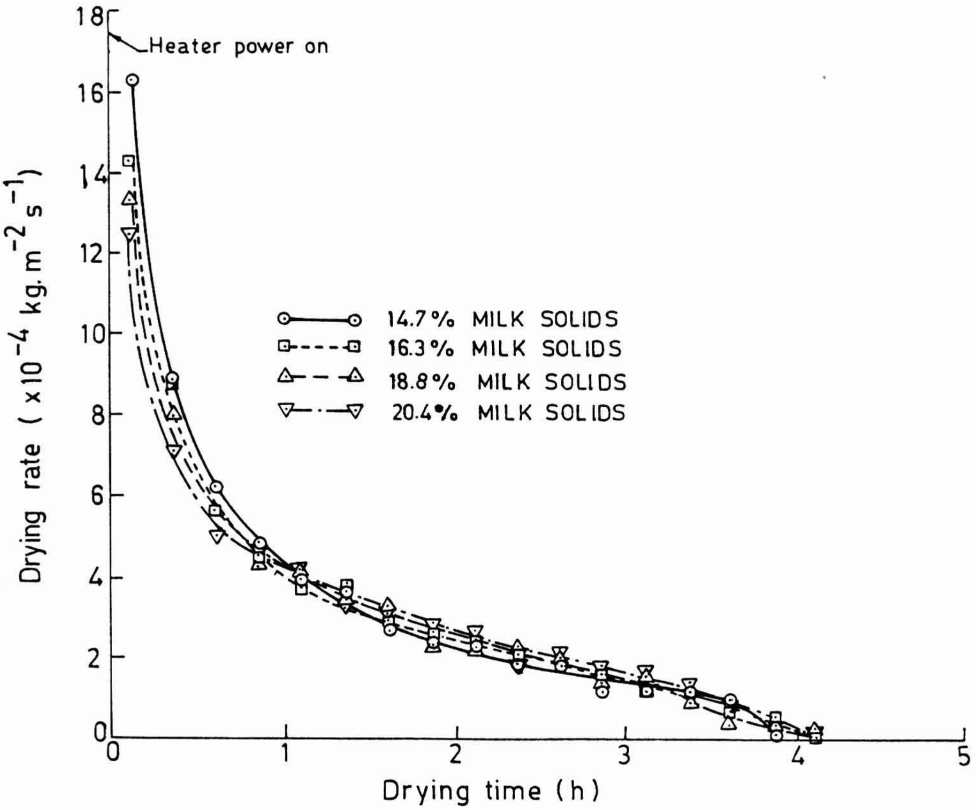

FIG. 3. DRYING RATE CURVES FOR YOGHURT CONTAINING DIFFERENT CONCENTRATION OF MILK SOLIDS

Apparently, a crust formation takes place in liquid foods during freezing, which offers additional resistance to vapor flow during the drying process. The formation of a surface film or crust in liquid foods has been documented by other researchers (Lambert and Marshall 1962; Quast and Karel 1968; Sagara 1984). Flink (1975) indicated involvement of carbohydrates in surface-film formation. The nonoccurrence of a constant-rate period in this study may be ascribed to this effect. Further, the shape of the drying curves is asymptotic, tending towards a linear drying rate as the drying progresses.

The production rate and drying time per unit output of freeze-dried yoghurt are shown in Fig. 4. With the increase in solids concentration in yoghurt from 14.7 to 20.4%, the production rate of freeze-dried yoghurt increased from 0.2196 to 0.3067 kg m^{-2} h^{-1} and the drying time per unit output decreased from 1.265 to 0.8658 h/g (Table 1). This shows an increase of 40.6% in the production rate

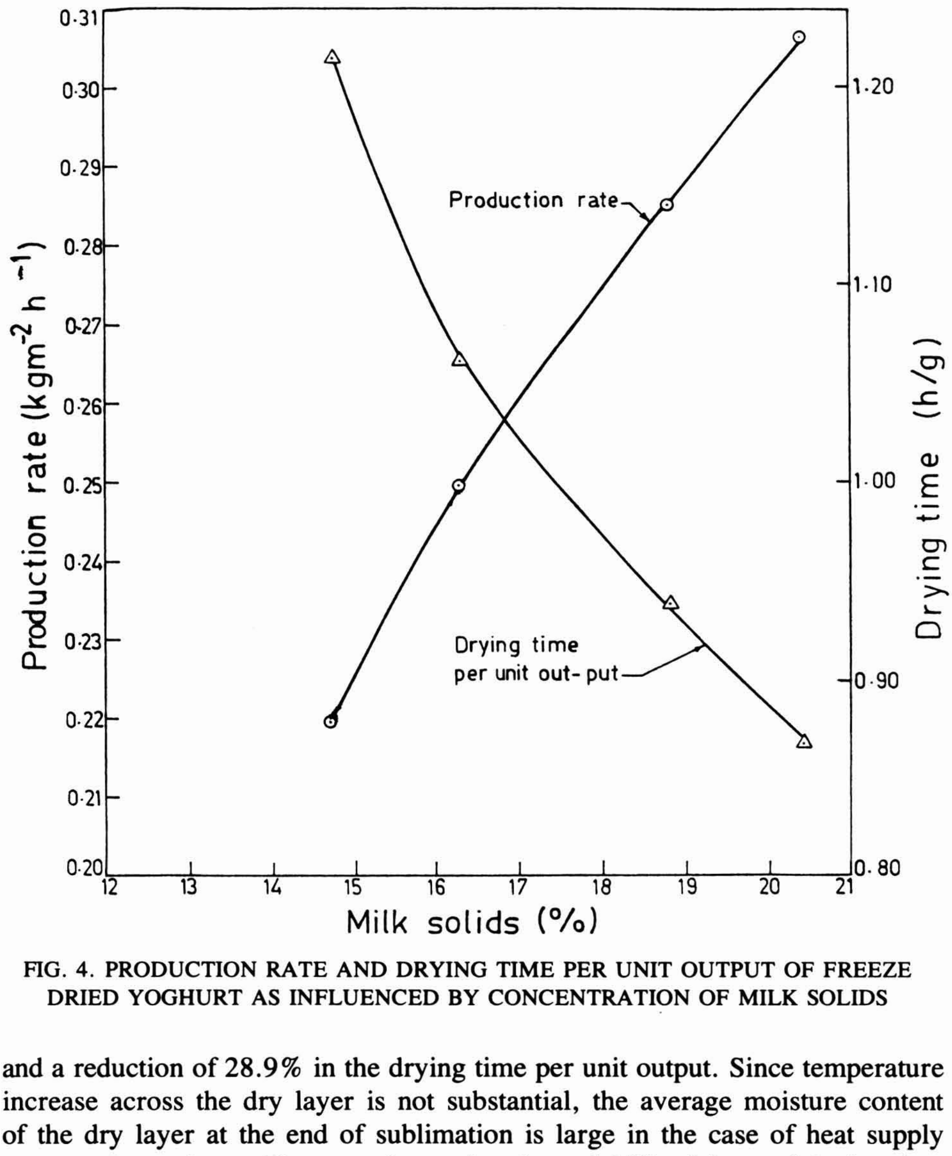

FIG. 4. PRODUCTION RATE AND DRYING TIME PER UNIT OUTPUT OF FREEZE DRIED YOGHURT AS INFLUENCED BY CONCENTRATION OF MILK SOLIDS

and a reduction of 28.9% in the drying time per unit output. Since temperature increase across the dry layer is not substantial, the average moisture content of the dry layer at the end of sublimation is large in the case of heat supply across a frozen layer. Hence, a desorption time of 66% of the total drying time was observed in this study. Earlier studies have also shown that desorption time may be as much as or more than the sublimation time (Sandall *et al.* 1967; King 1971; Aguilera and Flink 1974; Mellor 1978). Here desorption time is the dominant factor in determining the productivity of the process. Furthermore, the drying rate increases with the increase in the solids concentration during desorption.

TABLE 1.
INFLUENCE OF CONCENTRATION OF MILK SOLIDS IN YOGHURT ON THE PRODUCTION RATE AND THE DRYING TIME

Concentration of milk solids %	Drying time/ unit output h /g	Reduction in drying time %	Production rate Kg $m^{-2}h^{-1}$
14.7	1.2650	-	0.2196
16.3	1.0718	15.27	0.2495
18.8	0.9380	25.85	0.2851
20.4	0.8658	31.56	0.3067

TABLE 2.
PROXIMATE COMPOSITION OF FREEZE-DRIED YOGHURT AT DIFFERENT CONCENTRATIONS OF MILK SOLIDS*

Conc.of solids in yoghurt	freeze-dried yoghurt					
	Moisture	Protein	Fat	Lactic acid	Ash	Bulk density
(%)	(%)	(%)	(%)	(%)	(%)	(g/cm^3)
14.7	4.3	26.3	29.8	5.80	5.02	0.29
16.3	4.5	26.8	28.0	6.52	5.38	0.32
18.8	5.3	27.6	23.1	6.61	5.51	0.40
20.4	5.9	30.5	20.2	6.95	6.33	0.42

* Average of three determinations

Therefore productivity increases more than that accounted for by the lower amount of water needed to be evaporated. With the increase in solids concentration, the eutectic temperature decreases and partial melting of the frozen core during drying may occur. Secondly, yoghurt being a cultured product, the sensory characteristics of the freeze-dried product will be a limiting factor in deciding the solids concentration in yoghurt.

Table 2 shows the proximate composition of freeze-dried yoghurt samples prepared using different concentration of solids in milk. Freeze-dried yoghurt prepared from whole cow milk contained 26.3% protein, 29.8% fat and 5.02% ash. As expected, the addition of NFDM at 2, 5 and 8% levels enhanced protein and ash content of the products, whereas their fat contents decreased. The concentration of lactic acid in the freeze-dried product increased from 5.8 to 6.95, and the average bulk density increased from 0.29 to 0.42 g/cm³. Vitanov *et al.* (1973) also reported similar values for different constituents of freeze dried

Bulgarican yoghurt. However, they obtained a value of 15.1% for fat content of freeze-dried yoghurt compared to 20.2–29.8% obtained in this investigation. This may be attributed to low-fat milk used for yoghurt preparation by these authors.

The acceptability of freeze-dried yoghurt samples was determined after reconstitution. The acceptability scores of the samples prepared from yoghurt containing 14.7, 16.3, 18.8 and 20.4% total solids were 5.08, 6.50, 7.58 and 6.41, respectively. Analysis of variance showed that the samples differed significantly ($P < 0.05$). The magnitude of difference among samples was determined by Tukey's Test analysis (Table 3). The data show that the samples containing 16.3 to 20.4% solids were superior ($P < 0.05$) to the sample containing 14.7% solids (without added NFDM). However, no significant difference among samples containing 16.3 and 20.4% solids was observed. It was also observed that increasing the level of solids in milk up to 18.8% improves the acceptability of the product. A further increase in concentration of solids lowers the acceptability of the product. The panelists recorded that such samples are characterized by chalkiness.

The results of this investigation show that increasing the milk solids in yoghurt enhances the yield of the freeze-dried product and reduces the drying time per unit output. A reduction of 25.8% in drying time per unit output was observed as the concentration of solids increased from 14.7 to 18.8%. A further increase in solids concentration in yoghurt from 18.8 to 20.4% resulted in 5.7% reduction in drying time. Organoleptic evaluation of the product revealed that acceptability of the product improved up to the 18.8% level of solids concentration. A further increase in the concentration of solids impairs the sensory attributes of the product.

TABLE 3.
TUKEY'S TEST ANALYSIS

Acceptability	C	B	D	A
Score	7.58	6.50	6.42	5.08
S.E.	0.15			
L.S.D.	0.15x3.67*=0.55			
Difference among samples	C-B=1.08> 0.55 C-D=1.16> 0.55 C-A=2.50> 0.55 B-D=0.08< 0.55 B-A=1.42> 0.55 D-A=1.34> 0.55			

*Table values for 3 treatments and 15 d.f.for error
Sample A,B,C and D contained 14.7%, 16.3%, 18.8% and 20.4% milk solids respectively.

ACKNOWLEDGMENTS

The authors thank Professor B.P.N. Singh, Dean, College of Technology, for help in interpretation of the experimental data and Dr. S.K. Verma Department of Animal Science for providing the freeze dryer. The authors also gratefully acknowledge the assistance of Dr. F.W. Bakker-Arkema (Professor of Agricultural Engineering, Michigan State University), in the preparation of this manuscript.

REFERENCES

AGUILERA, J.M. and FLINK, J.M. 1974. Technical note: determination of moisture profiles from temperature measurements during freeze drying. J. Food Technol. *9*, 391–396.

AOAC. 1980. *Official Methods of Analysis*, 13th ed. Association of Official Analytical Chemists, Washington, D.C.

APHA. 1972. *Standard Methods for the Examination of Dairy Products*, 12th ed. American Public Health Association, Washington, D.C.

BLANCHAUD, M. 1972. Fermented milk based food and its preparation. French Pat. 20,9,3908.

DEETH, H.C. and TAMINE, A.Y. 1981. Yoghurt: nutritive and therapeutic aspects. J. Food Protect. *44*, 78–86.

FLINK, J.M. 1975. Applications of freeze-drying for preparation of dehydrated powders from liquid food extract. In *Freeze Drying and Advanced Food Technology*, (S.A. Goldblith, L. Rey and W.W. Rothmay, ed.) pp. 309–327, Academic Press, London.

FRANKS, F. 1989. Improved freeze-drying: an analysis of the basic scientific principles. Process Biochemistry.

GAVIN, M. 1968. Freeze drying of yoghurt. Schweiz. Milchztg. (Lait Romand) *94*(57), 455–458.

I.S.I. 1981. *Handbook of Food Analysis Dairy Products*, SP Part XI, Indian Standards Institution, New-Delhi.

KING, C.J. 1971. *Freeze-Drying of Foods*, p. 17, CRC Press, Cleveland, Oh.

KUMAGAI, H., NAKAMURA, K. and TOSHIMASA, Y. 1984. Proceedings Fourth International Drying Symposium, pp. 413–417, Kyoto, Japan.

LAMBERT, J.B. and MARSHALL, W.R. Jr. 1962. *Freeze-Drying of Foods*, (F.R. Fischer, ed.), National Academy of Sciences, National Research Council, Washington, D.C.

LARMOND, E. 1977. Laboratory Methods for Sensory Evaluation of Foods. Canada Department of Agriculture Publication 1637, Ottawa.

McDONOUGH, F.E., HITCHINS, A.D. and WONG, N.P. 1982. Effects of yogurt and freeze-dried yogurt on growth stimulation of rats. J. Food Sci. *47*, 1463–1465.

MELLOR, J.D. 1978. *Fundamentals of Freeze-Drying*, p. 71, Academic Press, New York.

QUAST, D.G. and KAREL, M. 1968. Dry layer permeability and freeze-drying rates in concentrated fluid systems. J. Food Sci. *33*, 170–175.

RADAEVA, I.A., KOCHERGA, S.I., SHULKINA, S.P. and EFRON, B.G. 1970. 18th International Dairy Congress, I.E., p. 408.

SAGARA, Y. 1984. Transport Property Measurement of a Food Sample Undergoing Sublimation Dehydration. Proceedings of Fourth International Drying Symposium, pp. 413–421, Kyoto, Japan.

SANDALL, O.C., KING, C.J. and WILKE, C.R. 1967. The relation between transport properties and rates of freeze-drying in poultry meat. A.I.Ch.E.J. *13*, 428–438.

SAVAIANO, D.A. and LEVITT, M.D. 1984. Nutritional and therapeutic aspects of fermented dairy products A.S.D.C. J. Dentistry Child. *51*(4), 305–308.

TAMIME, A.Y. and ROBINSON, R.K. 1985. *Yoghurt: Science and Technology*, Pergamon Press, New York.

TOEI, R. 1984. Developments in Spray, Freeze and Agitated Indirect Heat Drying. Proceedings of Fourth International Drying Symposium, pp. 880–887, Kyoto, Japan.

VIETZ, L. 1966. Freeze drying of yoghurt. Nova Proizv *17*, 262 (Dairy Sci. Abstr. *30*, No. 2617).

VITANOV, T., NIKOLOV, N. and BOYDASHEVA, L. 1973. *Proceedings of 13th International Congress of Refrigeration*, (W.T. Pentzer, ed.) pp. 773–779, Van Nostrand/AVI, New York.

WINWOOD, J. 1987. The living world of Yoghurt. Food Manuf. *62*(6), 39–43.

PRACTICAL FLUIDS FOR FOOD RHEOLOGY AND PROCESS ENGINEERING STUDIES

M. HULL

A.E. Staley Manufacturing Company
Decatur, Illinois

and

J.F. STEFFE[1]

Department of Agricultural Engineering
Department of Food Science and Human Nutrition
Michigan State University
East Lansing, MI

Accepted for Publication March 16, 1992

ABSTRACT

Corn syrups were shown to have potential for use as Newtonian calibration fluids in some applications where established standard oils are not suitable. Rheological analyses, using both steady and dynamic shear conditions, demonstrated that corn syrup viscosities are as constant as those of standard calibration oils. Some syrups showed significant elasticity that may be due to their tendency to dry upon exposure to air during testing. With careful attention to shelf-life and protection from air drying, corn syrups can be used in many food engineering problems where equipment calibration and process standardization are needed.

INTRODUCTION

Calibration is carried out to ensure that an analytical method gives accurate results. Fluids traditionally used for day-to-day calibration of rheometers are various oils and other polymers. These include all of the materials provided by

---

[1] Address correspondence to: J.F. Steffe, 209 Farrall Hall, Michigan State University, East Lansing, MI 48824-1323.

Journal of Process Engineering **15** (1992) 199–212.

national standards laboratories (Marsh 1980): mostly Newtonian oils, with viscosities that are constant at a given temperature and pressure. These fluids are secondary to water, the primary reference material for viscosity.

Few fluids have been cited in the literature as having been actually used or proposed as calibration materials for viscometry. Besides the water standard — petroleum oils, butene polymers, and silicone oils — only two other groups of fluids have been seriously considered as Newtonian calibration fluids. These can be classified as pure compounds and solutions.

Hardy (1962) noted that the use of pure chemicals as reference standards has been proposed in the scientific community. The rationale was that pure compounds could be characterized by a standards laboratory, then confidently used in other laboratories after appropriate routine purification. Unfortunately, the techniques for both purification and checking purity of many potential calibration fluids were too specialized (Hardy 1962). By 1984, however, this situation had changed. Various organic solvents became available with remarkable purities (part per billion levels in some cases) to serve burgeoning applications in spectroscopy and chromatography. Bauer and Meerlander (1984) studied low viscosity (less than water) fluids with the aim of improving the reproducibility of measurements of the same fluid on different viscometers. They recommended several commercially available hydrocarbons and halogenated hydrocarbons for use as viscosity standards.

Few pure compounds that exist as fluids at 25C have viscosities above 0.1 Pa s (Weast 1990). The viscosity of glycerin is 0.954 Pa s but the material is hygroscopic (Stecher 1960). Glycerin shares, with other pure compounds, the limitation that several fluids of various viscosities are often needed for the many applications that require a range of conditions to be evaluated.

Most certified calibration fluids are solutions comprised of several different pure fluids. The only solid-in-liquid solution proposed as a calibration material is sucrose-water (Bates 1942; Andrade 1947). However, numerous problems with this material were cited: solution purity from dust (filtering would change the concentration), condensation and evaporation, the need to prepare solutions the day of use, and applications in a limited temperature range (15–25C) were cited. With high concentrations of sucrose, the solution viscosity can change 25% for a 1% change in sucrose concentration. Since most liquid sugar syrups sold to the food industry in the U.S. are 67% sucrose (Hoynak and Bollenback 1966), preparing and using sucrose solutions above about 0.4 Pa s involves considerable inconvenience and potential error.

Polymers tend to form aqueous solutions that are non-Newtonian (Szczesniak and Farkas 1962). Most polymers are very large, entangled in solution, and increasingly align and deform in the direction of rising rates of shear. Some polymers exhibit little of this behavior if they are relatively small and do not form secondary associations with their polymer neighbors in solution. Many corn syrups are solutions of such polymers, along with smaller saccharides. Currently, a very wide range of corn syrup viscosities are available (up to 170 Pa s at 25C) at low cost.

Many applications in the food industry (laboratory viscometers requiring substantial sample volume of material, tube viscometers beyond capillary size, process viscometers, mixers, pumping equipment, manifolds, filters and screens, most heat exchangers, and extruders) requiring calibration fluids are not well-served by the current recognized standards. Some problems require fluids with a viscosity several orders of magnitude above the 0.001 Pa s value of water. High cost limits practical use to small volume viscometers found in the laboratory. All require organic solvents for cleaning with the higher viscosity standards being readily soluble only in halogenated hydrocarbons such as chloroform. There exists a need for calibration fluids that are inexpensive, well-characterized, reasonably Newtonian in behavior, stable, easily cleaned with water, and suitable for use in food processing.

While several investigators have published research using noncertified fluids as viscosity standards, none has studied the fluids *per se*. The limits of Newtonian behavior for many of these alternative fluids are unknown. Hence, the objectives of this study were: (1) to identify suitable calibration fluids for food industry use with regard to Newtonian flow behavior and ease of use, and (2) to determine the extent of Newtonian behavior of suitable fluids.

MATERIALS AND METHODS

Materials

ASTM viscosity calibration oils were obtained from Cannon Instrument Co., State College, PA. Corn syrup samples were donated by A.E. Staley Co., Decatur, IL. The approximate viscosities of the test fluids are listed in Table 1.

Equipment

Two rheometers were operated to evaluate fluid behavior. A Haake RV12 (Fisons Instruments, Paramus, NJ) with M-150 and M-500 sensors, and the SV and MV concentric cylinder sample fixtures, was used for steady shear experiments. The ratio of the diameter of the inner rotating cylinder to the outer fixed cylinder ranged from 0.955 to 0.873. The outer cylinder was fitted with a cap to help exclude air from the top of the sample. A Carrimed CS500 (Carrimed, Ltd., Dorking, England) was used for both steady and dynamic oscillatory

TABLE 1.
APPROXIMATE VISCOSITIES OF TEST FLUIDS

Fluid Type	Fluid Name	Viscosity at 25 C, Pa s
oil	S 60	0.1
oil	S 600	1.4
oil	S 8000	21
oil	S 30000	77
corn syrup	Isosweet 100	0.17
corn syrup	Isosweet 5500	0.80
corn syrup	Staley 4300	17
corn syrup	Neto 7350	47
corn syrup	Sweetose 4400	87
corn syrup	Staley 1300	87
corn syrup	Staley 300	170

experiments. The sample fixture geometry was cone and plate with the following cone angles and radii: 1°-2cm, 2°-2cm, 2°-1cm and 2°6cm. The "solvent trap" on the Carrimed was used in the corn syrup analyses to effectively exclude air from the sample surface. A concentric solvent trap well (Fig. 1) was filled with water to effect the seal. All measurements were made at 25.0 ± 0.2C. Calculations to determine rheological properties were performed using standard techniques (Whorlow 1980).

Approach

The research focused on comparisons of the corn syrups with the ASTM calibration oils, which are generally accepted as Newtonian. Comparisons were made with respect to the degree of Newtonian performance in steady shear, dynamic shear, time and shear dependency, and handling stability.

Steady Shear

Fluids were subjected to continuously increasing shear rates while the resulting shear stress was measured. A variation of this approach is to immediately repeat the increasing shear rate program in the reverse order. The first part is called the "up-ramp" while the second part is called the "down-ramp." Tests were also conducted using the Haake rheometer where shear rates were incrementally increased, each "step" being held for 30 s before being rapidly changed to the next shear rate value. The shear stress readings in the final 16 s of the step were averaged. This step ramp program was designed to minimize errors due to sample fixture inertia and/or the deflection or "windup" of the torque-measuring

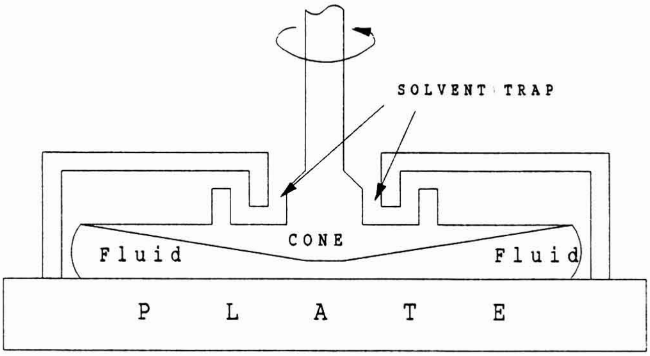

FIG. 1. CARRIMED CONE AND PLATE GEOMETRY
WITH SOLVENT TRAP

spring in the Haake rheometer. A correlation coefficient, r^2, was calculated from a straight line fit through each shear stress versus shear rate plot using the method of least squares.

Dynamic Oscillatory Shear

Fluids were tested using the Carrimed CS-500 rheometer to check for elastic behavior. Fluids are known to exist that are very elastic, yet whose steady shear viscosity does not change with shear rate (Boger 1977). Torque sweeps at constant frequency, as well as frequency sweeps at constant torque, were conducted. The amplitude of oscillation was automatically limited to 10 milliradians with programmed software control. Torque sweeps used a frequency of 0.5 Hz (in the logarithmic middle of the available range), while the frequency sweeps were conducted from 0.05 to 4.332 Hz, the widest efficient range available on the CS500.

Time-Shear Dependency

Time-dependent behavior was evaluated using an up-ramp immediately followed by a down-ramp in shear rate. A second approach taken was to simply perform a series of identical experiments on a sample without removal from the rheometer. Analyses were conducted after the sample was left in the rheometer for a period of one to several days, allowing for the possibility of structural recovery in the sample. Finally, samples were analyzed over a period of months to determine shelf stability.

TABLE 2.
LINEARITY OF SHEAR STRESS — SHEAR RATE ANALYSES AS EXPRESSED BY CORRELATION COEFFICIENT, CONCENTRIC CYLINDERS

Fluid	Shear Rate, s^{-1}	η, Pa s	r^2
	Continuous ramp data:		
Cannon S60	2 - 592	0.109	0.999
"	3 - 596	0.097	0.999
"	3 - 596	0.095	0.999
IsoSweet 100	3 - 478	0.173	0.999
"	3 - 478	0.175	0.999
	Step ramp data:		
Cannon S60	5 - 596	0.096	0.999
IsoSweet 100	2 - 478	0.178	0.999
Cannon S600	2 - 226.5	1.330	0.999
IsoSweet 5500	2 - 359.3	0.829	0.999
"	2 - 322.7	0.812	0.999
Cannon S30000	0.5 - 54.0	73.8	0.997
"	0.5 - 54.1	70.2	0.998
"	0.7 - 49.5	76.8	0.999
Neto 7350	0.9 - 76.6	51.9	0.997
"	0.9 - 76.0	47.2	0.997
"	1.0 - 76.2	53.3	0.998
Sweetose 4400	0.9 - 45.2	87.0	0.999
Staley 1300	0.9 - 44.9	82.7	0.999
"	0.9 - 45.3	87.2	0.999

TABLE 3.
LINEARITY OF SHEAR STRESS — SHEAR RATE ANALYSES RESULTS AS EXPRESSED BY CORRRELATION COEFFICIENT, CONE AND PLATE

Fluid	η, Pa s	r^2
IsoSweet 100	0.195	0.999
"	0.161	0.999
Cannon S600	1.25	0.999
"	1.12	0.999
"	1.29	0.999
"	1.29	0.999
Sweetose 4300	17.3	0.999
Staley 3260	19.9	0.999
"	19.4	0.999
"	17.4	0.999
Cannon S8000	18.7	0.999
"	17.6	0.999
Cannon S30000	77.8	0.999
"	78.3	0.999
"	74.9	0.999
Staley 4400	101.0	0.999

TABLE 4.
DYNAMIC OSCILLATION RESULTS FOR CANNON S8000 OIL AND STALEY 3260 SYRUP

	Cannon S8000 oil		Staley 3260 syrup	
Frequency (Hz)	G′, Pa	η', Pa s	G′, Pa	η', Pa s
0.0500	0.106	22.6	0.236	26.0
0.0661	0	23.0	0.281	25.7
0.0873	0	23.0	0.483	25.2
0.115	0.0221	22.7	0.551	24.6
0.153	0	22.5	0.700	24.8
0.202	0	21.9	1.12	24.4
0.266	0.0104	22.3	1.46	24.2
0.352	0	22.3	2.39	24.2
0.465	0	21.9	2.50	23.6
0.615	0.0329	22.1	3.99	23.7
0.813	0.954	22.3	4.52	23.9
1.07	0.0482	21.9	6.65	23.4
1.42	0.664	22.3	10.6	23.2
1.88	0	22.1	14.6	22.9
2.48	0	21.8	16.6	22.6
3.28	0	20.8	30.8	21.4
4.33	0	19.5	45.6	20.6

RESULTS AND DISCUSSION

Steady and Dynamic Shear

One measure of the Newtonian behavior of a fluid is the linearity (and zero intercept) of a shear stress versus shear rate plot. Table 2 and Table 3 compare the linearity and Newtonian viscosity (η) of the Cannon calibration oils with that of several corn syrups for analyses conducted using the concentric cylinder and cone and plate geometry, respectively. The corn syrup data are as linear as that of the calibration oils. None of the fluids tested exhibited a yield stress.

A comparison of dynamic test results of a standard oil and a syrup of similar viscosity shows some differences (Table 4). The data are somewhat erratic (due to the CS500's limited computer digital feedback control rate, significant instrument and fluid inertia, mechanical resonances, and slight sensor misalignment, phase angle near 90°, and imperfect Fourier transform of the measured in-phase component of the waveform), but the syrup did show increasing storage moduli (G′) values with increasing frequency, whereas the oil did not exhibit this behavior. One may conclude that while the corn syrup dynamic viscosity (η') was constant over the range studied, the material had a greater elastic component. One possible cause of this behavior was the drying of the syrup at the edge of the cone and plate fixture. Drying could occur despite use of the solvent trap accessory, since a brief interval was inescapably required to position the solvent trap after loading the syrup between the cone and plate. The dried syrup could show significant elasticity; no analogous structure would form when testing an oil.

Time and Shear-Dependency

The viscosity of an ideal fluid will not change as a result of being sheared or over time. A thixotropic loop is typically seen in fluids that break down during the first part of steady shear up-ramp, down-ramp analysis.

Typical flow curves for medium viscosity fluids are shown in Fig. 2. No significant thixotropic loop is evident from the graphs; the somewhat jagged curves are probably due to a slight warp or misalignment in the Carrimed fixtures. There is no difference in the general shape or separation of the loops between the Cannon calibration oil and the corn syrup of similar viscosity.

While high viscosity corn syrups behaved like the medium viscosity syrups in these thixotropic tests, a low viscosity syrup did not. Figure 3, comparing the Staley I.S. 100 syrup with a Cannon S60 standard oil, represents typical results. While the oil shows essentially no difference between the up and down curves, the syrup shows a down-loop that first drops below the up-loop at the higher shear rates, then crosses so that the down-loop is above the up-loop at the lower shear rates. This anomalous behavior is probably due to drying of the syrup at the edge of the cone and plate. The lowest viscosity fluids were analyzed without the benefit of a solvent trap.

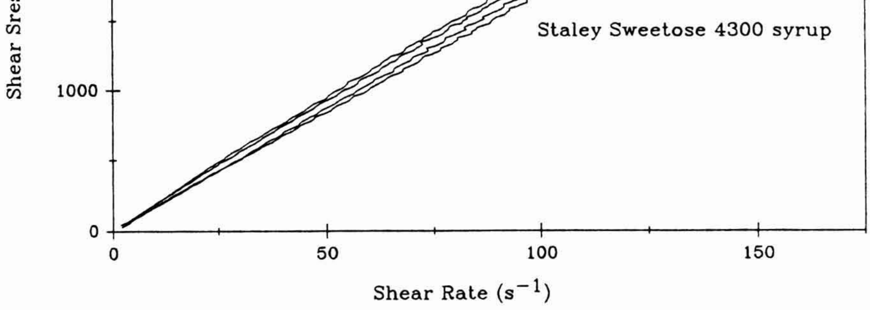

FIG. 2. FLOW CURVE COMPARISON OF SIMILAR VISCOSITY FLUIDS, CONE AND PLATE GEOMETRY

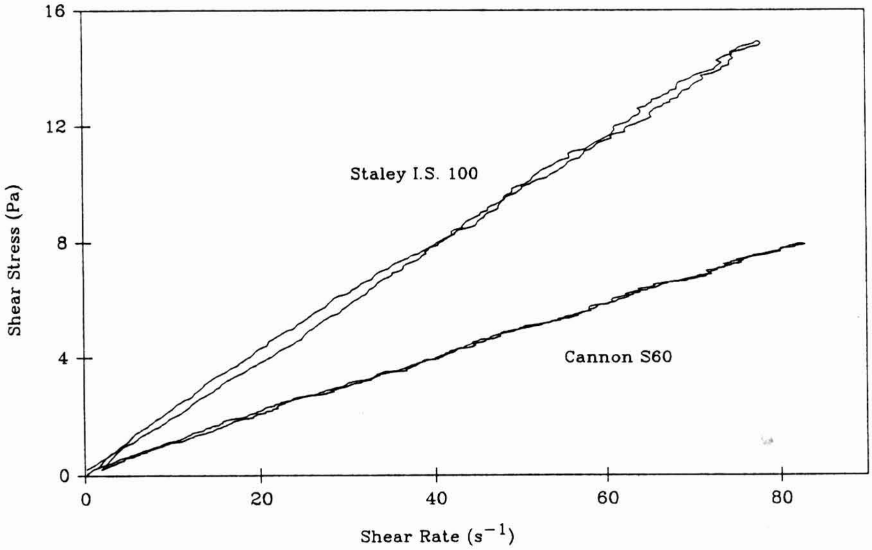

FIG. 3. FLOW CURVES WITH THIXOTROPIC LOOP OF LOW VISCOSITY FLUIDS, CONE AND PLATE

Time and shear-dependency were also tested by repeatedly analyzing the same sample without removal from the rheometer. A comparison of results for several fluids is found in Table 5. The table includes the Newtonian viscosity of each of several test runs performed on several fluids, as well as the percent difference by which subsequent results vary from the first result. All data reported are from the up-ramp part of the analysis only.

Standard calibration oils tended to decrease in viscosity with repeated analysis. The simplest explanation for this behavior is slight viscous heating during each analysis, a phenomenon in which some of the energy applied to cause flow was converted to heat, raised the temperature and thereby slightly lowered the viscosity for subsequent analyses. For example, data taken from the Cannon S8000 oil calibration certificate shows that an increase from 25.00C to 26.00C would result in a viscosity of 7.8%.

Corn syrups behaved differently than the standard oils (Table 5): oil viscosity decreased slightly with repeated analysis, while syrup viscosity increased slightly (except the Neto 7350 syrup, which was essentially unchanged). The syrups probably increased due to drying at the edge of the coaxial cylinders. This drying occurred despite use of a cover plate, positioned 5–10 mm above the top of rotating cylinder. The cover plate had a hole slightly larger than the rotor shaft, and certainly allowed some contact of the sample with circulating ambient air. The increase seen was small, but did point out the sensitivity of corn syrups to drying

TABLE 5.
RESULTS OF ANALYSES REPEATED ON SAME LOAD OF VARIOUS OILS AND SYRUPS, CONCENTRIC CYLINDERS

Fluid	run no.	η (Pa s)	% Difference
S60 oil	1	0.0977	
	2	0.0973	-0.4
	3	0.0977	0
I.S. 100 syrup	1	0.175	
	2	0.177	0.7
	3	0.177	1.1
S8000 oil	1	20.6	
	2	19.6	-4.7
	3	19.3	-6.3
Neto 7350 syrup	1	51.9	
	2	51.8	-0.1
	3	51.8	-0.1
S300000 oil	1	76.8	
	2	75.9	-1.2
	3	75.9	-1.2
1300 syrup	1	82.7	
	2	83.7	1.2
	3	84.6	2.4

during analysis. It is also possible that the syrups could absorb water both during transfer to the sample fixture and during testing. Perhaps the edge drying and moisture gain effects canceled each other out for the Neto 7350 syrup.

Fluids were analyzed over a period of time using steady shear in concentric cylinders. Samples (stored at 22C) were repeatedly analyzed for reach of several loadings each test day to avoid confounding the effect of sample load with that of different days. Student's t test (for comparison of a single pair) or Dunnett's t test (for multiple comparisons within a single fluid type) were used as $p < 0.05$ to compare analyses for a subsequent day with those obtained initially for a given type of fluid (Gill 1978). The Cannon calibration oils showed greater deviation from initial results, on subsequent days, than did the corn syrups (Table 6).

The Cannon fluids proved to be very stable during the typical manipulations required for laboratory experimentation over a period of months. The syrups, however, had some sensitivity to drying on exposure to air. A slight skin was noticeable at the fluid surface when transferring samples. Simply stirring the fluid prior to sampling seemed to alleviate any negative effects of the skin in the container itself. During analysis, the cone and plate geometry was quite susceptible to sample drying.

Effect of Sample Drying

Figure 4 shows a comparison of steady shear flow analyses performed on Sweetose 4300 syrup. The loop on the lower right results from an up- and down-ramp test using the solvent trap attachment for the cone and plate fixture. The syrup shows a slight thixotropic loop, as the down-ramp portion is below that of the up-ramp. The upper loop is the same syrup (different sample load) using the same cone, but without the solvent trap. The up-ramp curve turns up, almost certainly due to drying during the 30 s analysis period. Confirming this conclusion, the down-ramp curve is well above the up-ramp, showing such a large degree of drying that the viscosity (the slope of a line tangent to the curve at any point of interest) continues to increase as the torque is continuously decreased.

The large effect of the solvent trap discussed above was opposite in both trend and degree to that expected for a fluid that is not sensitive to air. One would expect a small amount of drag from the solvent held in the solvent trap well (Fig. 4). A test of potential effect of the solvent trap was made by first performing three successive up-down ramp analyses on one sample load of Cannon S8000. The solvent trap was then positioned without disturbing the sample between the cone and plate, and water was added to the trap well. A second set of three analyses was then conducted. The mean plus or minus one standard deviation for the "without trap" and "with trap" results (six results per trap status) were 22.02

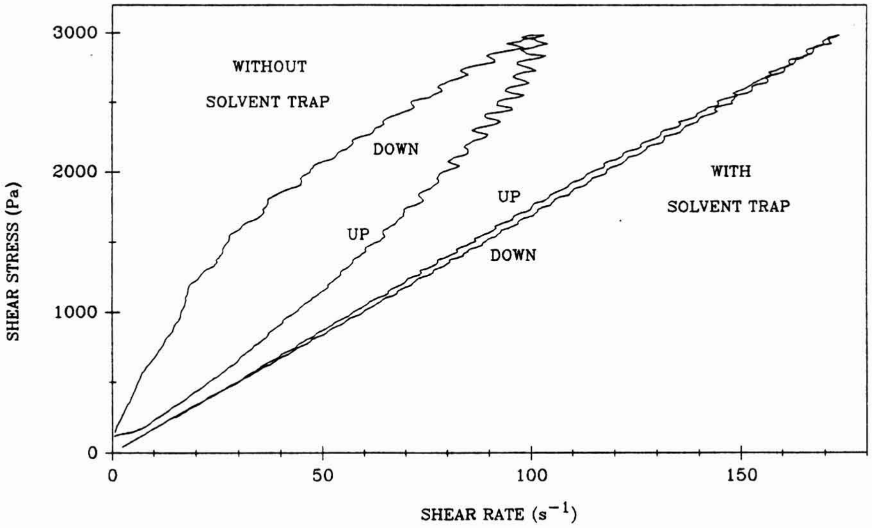

FIG. 4. FLOW CURVES OF STALEY SWEETOSE 4300 CORN SYRUP, EFFECT OF SOLVENT TRAP ON CONE AND PLATE RESULTS

TABLE 6.
RESULTS OF ANALYSES REPEATED ON DIFFERENT SAMPLE LOADS OF VARIOUS OILS AND SYRUPS, CONCENTRIC CYLINDERS

Fluid	Days After Test	Run no.	Up Ramp η (Pa s)	Avg η (Pa s)	% Diff.	Sig. Diff.?
S60 oil	0	1	0.109			
	126	1	0.0977			
		2	0.0973			
		3	0.0977	0.0976	-10.0	yes
	146	1	0.0952			
		2	0.0951			
		3	0.0960			
		4	0.0959	0.0956	-11.9	yes
I.S. 100 syrup	0	1	0.173			
		2	0.175	0.175		
		3	0.177			
		4	0.177	0.177		
	20	1	0.179			
		2	0.178	0.179		
		3	0.178			
		4	0.179	0.179	-1.3	yes
S30000 oil	0	1	73.8			
		2	72.8			
		3	72.1	72.9		
		4	70.2			
		5	69.6			
		6	69.1	69.7		
	95	1	76.8			
		2	75.9			
		3	75.9	76.2	6.9	yes
	138	1	78.1			
		2	77.4	77.7	9.1	yes
Neto 7350 syrup	0	1	51.9			
		2	51.8			
		3	51.8	52.8		
		4	47.2			
		5	46.4	46.8		
	185	1	53.3			
		2	53.7			
		3	51.5			
		4	54.7	53.3	0.9	no

± 0.47 and 21.49 ± 0.43, respectively. These means are not significantly different in a t test at $p = 0.05$. The trend in the data is unexpected, and may be due to slight sample loss or warning of the sample.

The stability of corn syrup viscosity over extended periods of time was not systematically studied. Some of the high fructose syrups require storage above ambient to minimize crystallization and "color development." A.E. Staley Co. recommended that Isosweet 100 be stored at 35–40.5C. Samples stored at 22C did form crystals, but these were dissolved by heating at 37C overnight. The data presented in Table 6 suggest that most syrups should have stable viscosities for several months.

SUMMARY

Corn syrups were shown to have potential for use as Newtonian calibration fluids in some applications where the established standard oils are not suitable. The syrups tested have viscosities as constant with varying shear rate as those of standard ASTM calibration oils. Some syrups showed significant elasticity that may be due to their tendency to dry upon exposure to air. Appropriate precautions in handling and analysis reduced this effect to insignificant levels for most practical food industry purposes.

Those wishing to use syrups as calibration fluids should carefully characterize the material with respect to the following: steady shear viscosity and temperature sensitivity, elasticity, sensitivity to air drying, and shelf-life. Also, the application should be characterized with regard to needed viscosity and temperature range, fluid exposure to air, and the length of time needed to conduct the calibration.

REFERENCES

ANDRADE, E.N. DA C. 1947. *Viscosity and Plasticity*, Cambridge University Press, Cambridge, England.

BATES, F.J. 1942. Polarimetry, saccharimetry and the sugars. Circ. NBS C440. U.S. Govt. Printing Office, Washington, DC.

BAUER, H. and MEERLANDER, G. 1984. Precise viscosity measurements of Newtonian liquids with $\nu < 1$ mm^2/s for the selection of suitable standards. Rheol. Acta *23*, 514–521.

BOGER, D.V. 1977. A highly elastic constant-viscosity fluid. J. Non-Newt. Fluid Mech. *3*, 87–91.

GILL, J.L. 1978. *Design and Analysis of Experiments in the Animal and Medical Sciences*, The Iowa State University Press, Ames.

HARDY, R.C. 1962. *NBS Viscometer Calibrating Liquids and Capillary Tube Viscometers*, Natl. Bur. Stand. (U.S.) Monograph 55.

HOYNAK, P.X. and BOLLENBACK, G.N. 1966. *This is Liquid Sugar*, Refined Syrups and Sugars, Yonkers, NY.

MARSH, K.N. 1980. Recommended reference materials for realization of physicochemical properties: section viscosity. Pure Appl. Chem. *52*, 2393–2404.

STECHER, P.G. 1960. *The Merck Index of Chemicals and Drugs*, 7th ed., Merck and Co., Rahway, NJ.

SZCZESNIAK, A.S. and FARKAS, E. 1962. Objective characterization of the mouthfeel of gum solutions. J. Food Sci. *27*, 381–385.

WEAST, R.C. 1990. *Handbook of Chemistry and Physics*, The Chemical Rubber Co., Cleveland.

WHORLOW, R.W. 1980. *Rheological Techniques*, Ellis Horwood Limited, Chichester; John Wiley & Sons, New York.

INFLUENCE OF PARTICLE ORIENTATION ON THE EFFECTIVE ELECTRICAL RESISTANCE AND OHMIC HEATING RATE OF A LIQUID-PARTICLE MIXTURE[1]

SUDHIR K. SASTRY[2] and SEVUGAN PALANIAPPAN

The Ohio State University
Department of Agricultural Engineering
590 Woody Hayes Drive
Columbus, OH 43210

Accepted for Publication May 28, 1992

ABSTRACT

The ohmic heating rate of a liquid-particle mixture is expected to depend on particle orientation. A mathematical model was developed to determine the extent of orientation dependence for the case of a cubic particle. The particle and liquid resistances were determined by taking incremental sections through the particle and using the electrical conductivity to calculate the effective resistance. Modeling and experimental results indicate that for a cubic particle, orientation effects are slight; both with regard to effective resistance and heating time. However, this result is not expected to apply to particles of large aspect ratios.

INTRODUCTION

Ohmic heating of liquid-particle mixtures is of relatively recent industry interest, but shows considerable promise for continuous sterilization of liquid-particle mixtures. Since heating is accomplished by passing an electrical current through the product, it is essential that the electrical conductivities of each phase, as well as the effective conductivity and resistance of the mixture, be known for purposes of process design. Since electrical resistance depends on the length and

---

[1] Salaries and research support provided by State and Federal Funds appropriated to the Ohio Agricultural Research and Development Center, The Ohio State University. Journal Article No. 87-92. References to commercial products and trade names is made with the understanding that no discrimination and no endorsement by The Ohio State University is implied.

[2] Corresponding author.

Journal of Process Engineering **15** (1992) 213-227. *All Rights Reserved.*

cross-sectional area of the conductor, particle orientation effects could be significant, as illustrated by de Alwis and Fryer (1990) for a long rectangular particle. Sterilization process design criteria must account for extreme cases, hence it is necessary to understand which particle orientations represent extremes of resistance. Since a particle may be oriented in infinitely many ways, the problem is tedious but fortunately lends itself to precise mathematical treatment. Several models exist in the literature for determination of electrical and thermal conductivities of two-phase mixtures (Maxwell 1881; Meredith and Tobias 1960; Kopelman 1966; Brailsford and Major 1964, among others); however these apply only to dilute spherical particle dispersions. A detailed discussion and evaluation of these models is provided by Palaaniappan and Sastry (1991).

The present paper is aimed at mathematical determination and qualitative experimental verification of the resistance of a cubic particle under various orientations relative to the current, as well as the effective resistance of a system consisting of a particle within a cylindrical sample of fluid of different conductivity. The results are expected to be useful in studies on modeling of heat transfer during ohmic heating.

MATERIALS AND METHODS

Mathematical Model

The coordinate axes of rotation are as specified in Fig. 1, with the y-axis assumed to be the direction of the electric field. The particle (a cube of side l) can rotate about any of these axes; however, rotations about the y-axis do not change the effective resistance, and may be considered redundant. Rotation about the x-axis (θ rotation) causes different cross sections to be exposed to the current; however identical repeating patterns are obtained every for 45° rotation; thus consideration of one 45° rotation is sufficient. By similar reasoning, only a 45° rotation about the z-axis (ϕ rotation) need be considered. For convenience, we will consider all positions to consist of first a θ rotation, followed by a ϕ rotation. For calculation of resistance of a solid in a liquid, the particle is assumed to reside within a cylinder of fluid of diameter equal to the diagonal dimension of the cube (i.e., $\sqrt{3}l$, so that the particle can always be contained within the circle.

In all cases, (except where unnecessary), the resistance of the particle can be considered as the sum of an infinite number of infinitesimally thin resistances, or:

$$R = \int_0^y dR = \int_0^y \frac{dy}{A(y)\sigma_s} \qquad (1)$$

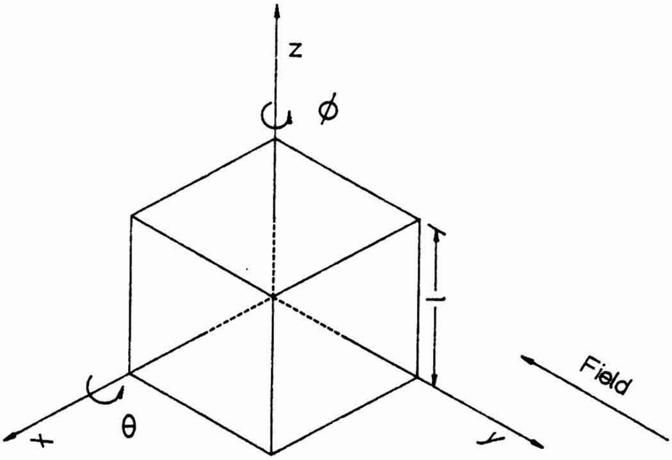

FIG. 1. ISOMETRIC VIEW OF CUBE SHOWING AXES AND ANGLES OF ROTATION

or, approximately:

$$R = \sum_{n=1}^{N-1} \bar{R}_n = \sum_{n=1}^{N-1} \frac{\Delta y}{\bar{A}_n \sigma_s} \tag{2}$$

where

$$\bar{A}_n = \frac{A_{n+1} + A_n}{2} \tag{3}$$

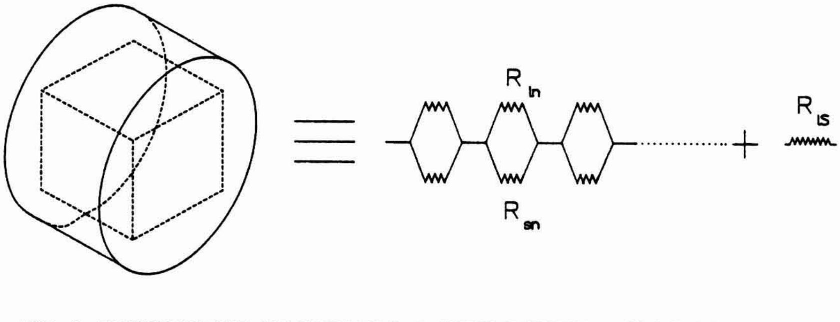

FIG. 2. EQUIVALENT CIRCUIT FOR A CUBE WITHIN A CYLINDER OF FLUID

The problem then reduces to determination of A_n for each specific situation. For calculation of solid-liquid mixture resistance, the circuit is considered as the sum of an infinite number of parallel solid-liquid circuits connected in series with each other and in series with a pure liquid resistance (Fig. 2). Mathematically speaking, this is approximated as:

$$R_m = R_{lS} + \sum_{n=1}^{N} \frac{\overline{R}_{ln}\overline{R}_{sn}}{\overline{R}_{ln} + \overline{R}_{sn}} \tag{4}$$

$$R_{lS} = 4(\sqrt{3}l - l_{max})/(3\pi l^2\sigma_l)$$

where

l_{max} = maximum length of particle in direction of field.

The problem then breaks down into a number of cases, each involving determination of A_n.

Case I. Particle Face Towards the Current

In this trivial case, the full face of the particle is oriented towards the current; consequently the cross-sectional area is l^2, and the length is l, yielding:

$$R = \frac{l}{A\sigma_s} = \frac{1}{l\sigma_s} \tag{5}$$

Case II. Particle with θ Rotation

Two situations occur, as illustrated in Fig. 3. In both cases, a rectangular cross section is exposed to the current; and the following relationships result.

Situation IIa

For $f \leq y_n \leq b$

$$A_n = l\left[\frac{l}{\sqrt{2}}\cos(45-\theta) - y_n\right]\tan\theta + \left[l\sin\theta + \frac{l}{\sqrt{2}}\sin(45-\theta) - y_n\right]\frac{l}{\tan\theta} \tag{6}$$

where $f = (l/\sqrt{2})\sin(45-\theta)$

$b = (l/\sqrt{2})\cos(45-\theta)$

Situation IIb

For $0 \leq y_n < f$

$$A_n = l^2\left(\cos\theta - \frac{1}{\sqrt{2}}\left[\sin(45-\theta) - \cos(45-\theta)\right]\right) \tag{7}$$

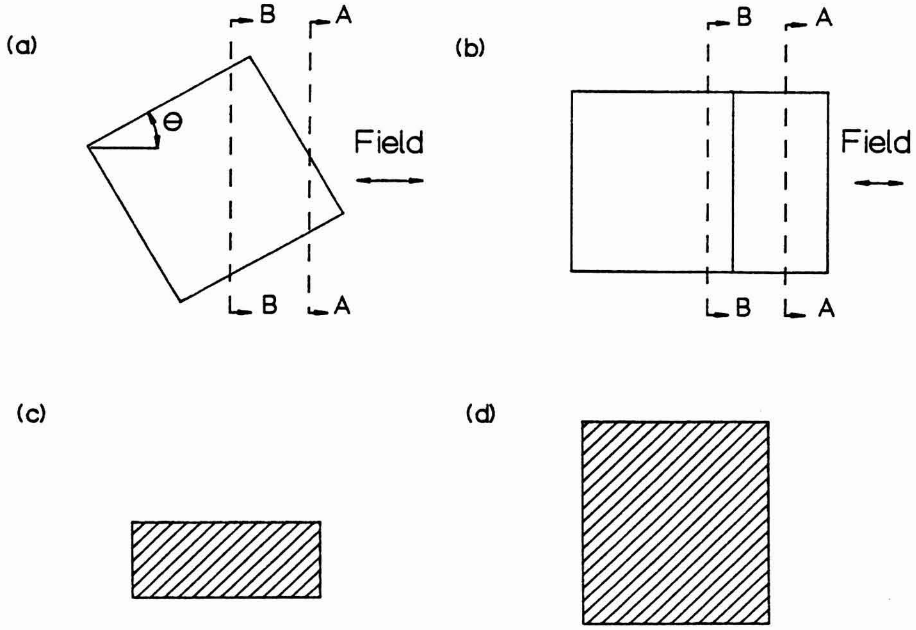

FIG. 3. ILLUSTRATION OF CASE II: PARTICLE WITH θ ROTATION ONLY
(a) Side evaluation; (b) plan; (c) section A-A; (d) section B-B.

Case III. Particle with Both θ and ϕ Rotations

This case, illustrated in Fig. 4(a), presents a number of possible scenarios, depending on the relative values of the corner coordinates k_1 through k_4. It is useful at this stage to determine their values in terms of l, θ and ϕ as:

$$k_1 = \sqrt{\frac{3}{4}}\, l \cos(\Psi - \theta_p)\cos(\Phi^- + \phi) \tag{8}$$

$$k_2 = \sqrt{\frac{3}{4}}\, l \cos(\Psi + \theta_p)\cos(\Phi^+ + \phi) \tag{9}$$

$$k_3 = \sqrt{\frac{3}{4}}\, l \cos(\Psi + \theta_p)\cos(\Phi^+ + \phi) \tag{10}$$

$$k_4 = \sqrt{\frac{3}{4}}\, l \cos(\Psi - \theta_p)\cos(\Phi^- - \phi) \tag{11}$$

where $\Psi = \tan^{-1}\{\tan(45)/\surd 2\}$

$\theta_p = \tan^{-1}\{\tan\theta/\surd 2\}$

$\Phi^+ = \tan^{-1}\{1/[\surd 2\cos(45+\theta)]\}$

$\Phi^- = \tan^{-1}\{1/[\surd 2\cos(45-\theta)]\}$

Situation IIIa

For max $[k_1, k_2] \leqslant y_n < k_4$ a triangular cross section occurs, as illustrated in Fig. 4(b).

$$A_n = \frac{[k_4 - y_n]^2}{2\cos^2\phi\,\sin\phi\,\cos\theta\,\sin\theta} \tag{12}$$

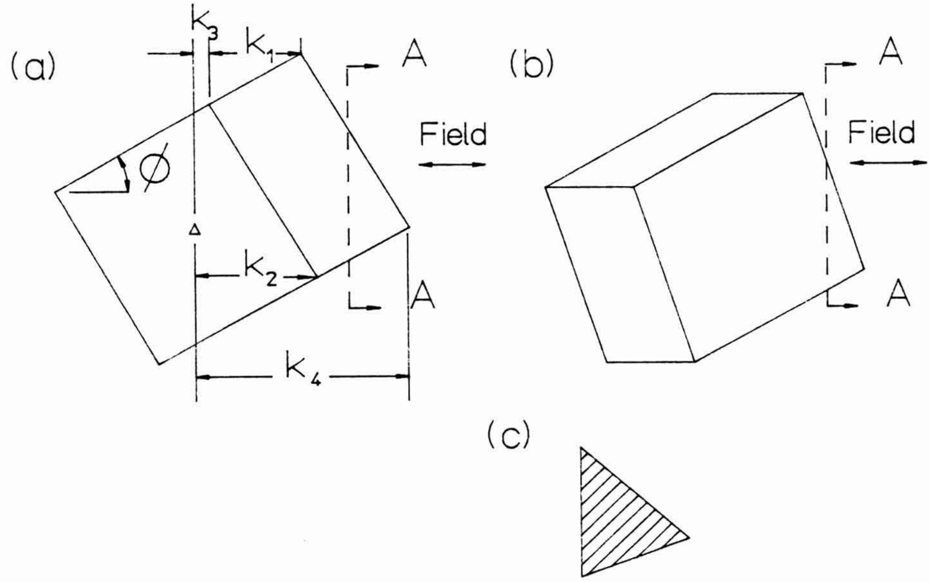

FIG. 4. ILLUSTRATION OF CASE III: PARTICLE WITH BOTH v AND ϕ ROTATIONS
(a) Plan; (b) side elevation; (c) section A-A, representing situation IIIa.

Situation III b

This occurs for min $[k_1, k_2] \leqslant y_n <$ max $[k_1, k_2]$. Three different situations can occur here, $k_1 > k_2$; $k_2 > k_1$; and $k_1 = k_2$. In the first 2 cases (Fig. 5), a trapezoidal cross-section is obtained in going from max $[k_1, k_2]$ to min $[k_1, k_2]$. For the third case, no trapezoidal zone occurs, and the situation is similar to III c, described later.

III b.1 $k_1 > k_2$, a trapezoidal cross section is obtained as in Fig. 5(a).

$$A_n = \frac{l[k_2 + k_4 - 2y_n]}{2\cos^2\phi \cos\theta \sin\theta} \tag{13}$$

III b.2 $k_2 > k_1$, a trapezoid, as in Fig. 5(b)

$$A_n = \frac{l[k_2 + k_4 - 2y_n]}{2\cos\theta \sin\phi \cos\phi_p} \tag{14}$$

where $\phi_p = \tan^{-1}\{\tan\phi/\cos\theta\}$

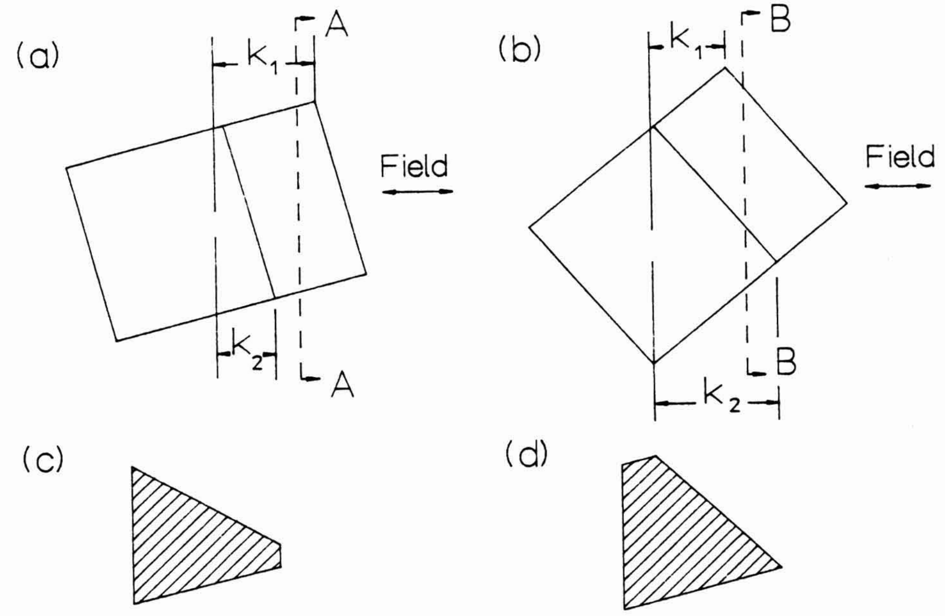

FIG. 5. ILLUSTRATIONS OF CASE III, SITUATIONS III b, SHOWING PLAN VIEWS AND SECTIONS
(a) $k_1 > k_2$; (b) $k_2 > k_1$; (c) section A-A; (d) section B-B.

Situation III c

This situation involves $k_3 \leqslant y_n < \min [k_1, k_2]$ as illustrated in Fig. 6(a), and produces a pentagonal cross section.

$$A_n = \frac{l}{2\cos\phi}\left[\frac{l}{\cos\theta} + l_1\left(\tan\psi_1 + \tan\psi_2\right) + \frac{k_1 - y_n}{\cos\phi\cos\theta\sin\theta}\right] - \frac{l_1^2}{2}\left[\tan\psi_1 + \tan\psi_2\right] \qquad (15)$$

where $l_1 = \{k_2 - y_n\}/[\cos\phi\sin\phi]$

$\psi_1 = \tan^{-1}[\tan\theta\sin\phi]$

$\psi_2 = \tan^{-1}[\cot\theta\sin\phi]$

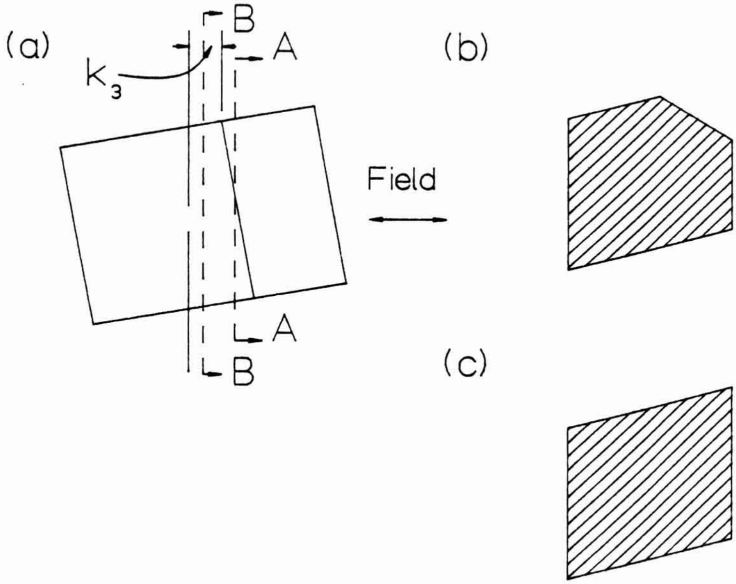

FIG. 6. ILLUSTRATIONS OF CASE III
(a) Plan; (b) section A-A, representing situation III c; (c) section B-B, representing situation III d

Situation III d

Here, $0 \leqslant y_n < k_3$; a parallelogram is obtained and A_n no longer depends on y_n.

$$A_n = \frac{l^2}{\cos\theta\cos\phi} \tag{16}$$

A FORTRAN program was written to perform the above computations over 1° increments in θ and ϕ from 0 to 45°. Calculations were performed for a range of solid-to-liquid conductivity ratios (r_c) ranging from 0.01 to 1 (σ_l was assumed equal to unity in all cases). Maximum, minimum and mean values of resistance were determined in each case, as were the orientations (θ and ϕ values) corresponding to the maximum and minimum resistance.

Experimental

Two potato cubes (0.01 m side) were placed within a fluid (0.1 M sodium phosphate solution) within a static ohmic heater (Fig. 7). Both particles were

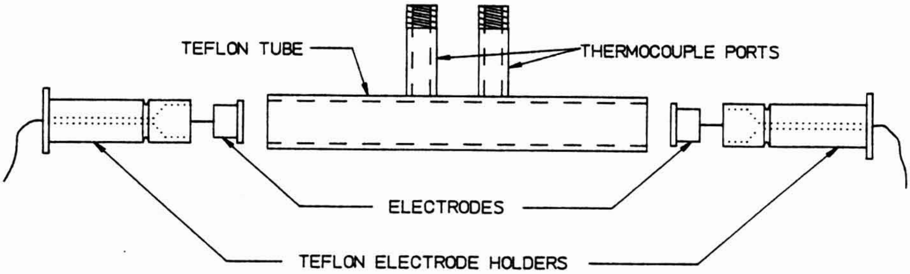

FIG. 7. EXPLODED VIEW OF EXPERIMENTAL SETUP

mounted at the desired orientation, (one attached to a teflon-coated thermocouple for internal temperature measurement). Samples were heated ohmically using a constant voltage, and temperatures of solid and liquid phases, voltage and current were monitored during the experiments. Since the purpose was primarily qualitative model verification, studies were conducted using two orientations only: one with particle face towards the current, and the other with a θ rotation of 45°.

RESULTS AND DISCUSSION

Results of model simulations are shown in Table 1, for various values of conductivity ratio r_c. In all cases, orientation had only a slight effect on the overall resistance of the mixture. As expected, for $r_c = 1$, orientation had no effect on the mixture resistance. As r_c decreased, the range of variation in resistance increased, but even at $r_c = 0.01$, the variation was less than 10%. The significance of orientation thus seems to increase as the conductivity ratio increases; however the effect is slight. Even at a conductivity ratio of 0.001, (far lower than likely to be encountered for liquid-solid mixtures), the variation was still found to be within 10%.

These findings can be qualitatively verified by Fig. 8, which shows the overall resistance of three potato-sodium phosphate mixtures versus temperature as affected by orientation. The results are similar, indicating the small effect of orientation in this case. The heating rates (Fig. 9) are also similar, indicating negligible orientation-related differences. Comparison between model results and experiment also yielded generally satisfactory prediction (Fig. 10) with only the results for the 0.5 M solution being offset slightly from predictions. This deviation may be due to sample-to-sample variation in electrical conductivity of particles.

TABLE 1.
MAXIMUM, MINIMUM AND MEAN VALUES OF RESISTANCE FOR VARIOUS CONDUCTIVITY RATIOS, AND θ AND ϕ VALUES CORRESPONDING TO THE MAXIMUM AND MINIMUM RESISTANCE ORIENTATIONS*

Conductivity Ratio (r_c)	Maximum			Minimum			Mean
	Resistance (Ω)	θ (°)	φ (°)	Resistance (Ω)	θ (°)	φ (°)	Resistance (Ω)
0.001	1.132	20	0	1.038	19	1	1.050
0.010	1.125	17	0	1.033	19	1	1.045
0.100	1.061	17	0	0.990	21	2	0.998
0.400	0.907	17	0	0.877	21	2	0.879
0.700	0.807	17	0	0.796	35	33	0.797
1.000	0.735	all	all	0.735	all	all	0.735

* - Based on a hypothetical cube side (l) of 1 m, and a liquid electrical conductivity of 1 S/m.

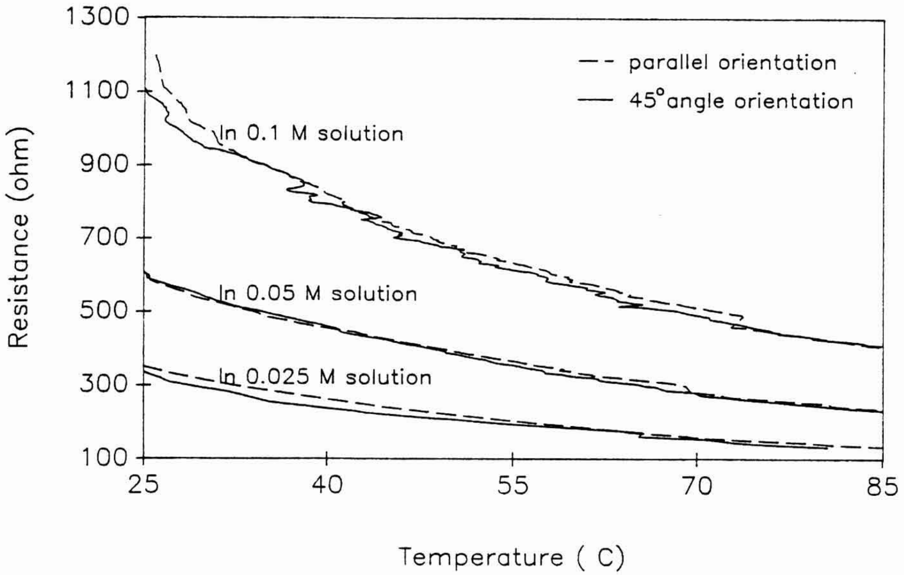

FIG. 8. PLOT OF MIXTURE RESISTANCE VERSUS TEMPERATURE FOR SODIUM PHOSPHATE SOLUTIONS CONTAINING POTATO PARTICLES ORIENTED PARALLEL AND AT 45° TO THE FIELD

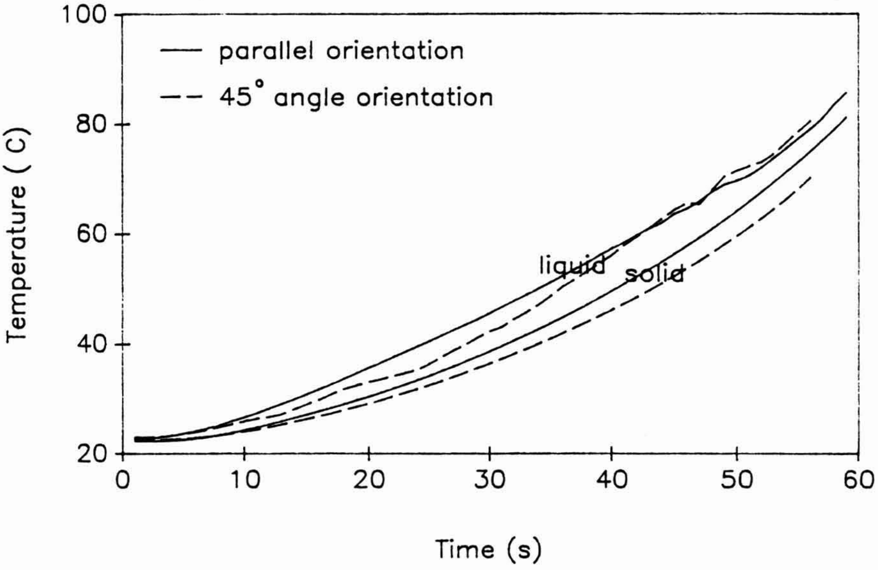

FIG. 9. PLOT OF LIQUID AND PARTICLE TEMPERATURE HISTORIES FOR PARALLEL AND 45° PARTICLE ORIENTATIONS

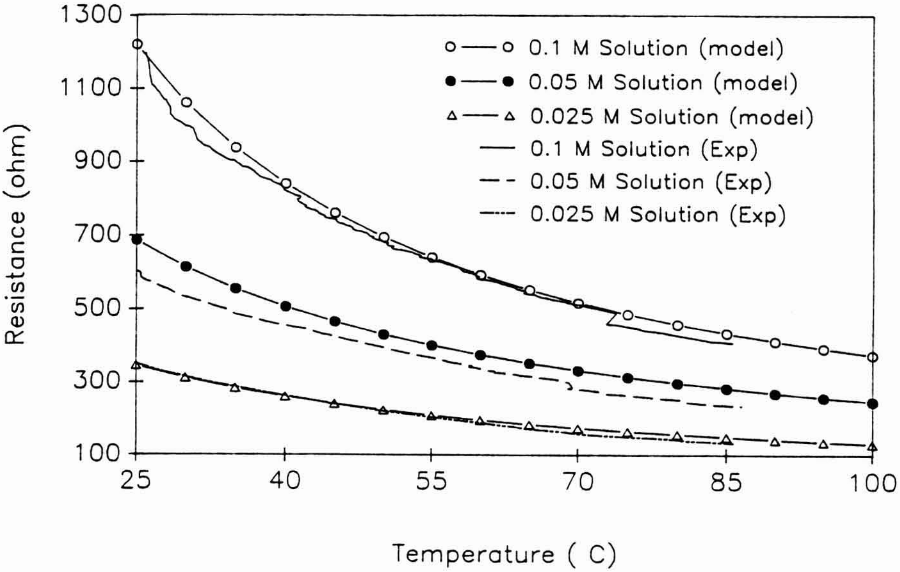

FIG. 10. PLOTS OF PREDICTED AND EXPERIMENTAL VALUES OF MIXTURE RESISTANCE VERSUS TEMPERATURES FOR VARIOUS POTATO-SODIUM PHOSPHATE SOLUTION MIXTURES

The absence of a pronounced orientation effect is primarily due to the aspect ratio of the particle, and the presence of a parallel (liquid) conduction path at all points. The resistance of a cube immersed in a nonconducting medium changes greatly with orientation if two corners were aligned with the current, due to the small cross-sectional area associated with the corners. This point has been observed in the present simulations.

While the present studies indicate small orientation effects for individual particles, it is by no means certain that this would be true if large particle populations are involved. In such situations, small variations in individual samples could result in large variations in the resistance of the population, due to a cumulative effect. This situation may occur with fine particle mixtures, where the particle population is large. Further work is necessary to test for such effects.

The primary implication of these results lies in the design of ohmic heating processes for particulates. If cubic particles of significant size are to be used, orientation effects can be considered small, and voltage gradients within the ohmic heater can be expected to show few local variations due to orientation. It must be noted, however, that our results apply to cubic particles alone, and not to particles of aspect ratio far from unity (long thin particles) such as those studied by de Alwis and Fryer (1990).

A final note pertains to the likelihood of local effects that may cause channeling of current. As discussed earlier, the presence of sharp edges or corners in an object creates a zone of high resistance, which results in low current density at these locations. This could well happen with cubic particles, resulting in low energy generation at the corners. Fortunately, these zones are also close to the fluid medium, and would be expected to heat more rapidly by convection than other locations. Further studies on such localized effects and on particles of large aspect ratios are necessary. The results of these studies do show that if particle shapes are carefully controlled, orientation effects can be minimized.

CONCLUSIONS

The effective resistance of a two-phase mixture consisting of liquid and a cubic particle shows only a slight dependence on orientation. The orientation effect increases as solid-to-liquid conductivity ratio increases, but the effect is not strong. This result is not applicable to cases involving long thin particles. Situations involving large particle populations merit further study.

NOMENCLATURE

A	Cross sectional area (m^2)
b	Dimension defined in text (m)
f	Dimension defined in text (m)
k_1	Dimension defined in text (m)
k_2	Dimension defined in text (m)
k_3	Dimension defined in text (m)
k_4	Dimension defined in text (m)
l	Side of cube (m)
n	Incrementing index
N	Total number of increments
R	Resistance (Ω)
r_c	Conductivity ratio (σ_s/σ_l)
x	Coordinate length (m)
y	Coordinate length (m)
z	Coordinate length (m)

Greek Letters

Δ	Increment
θ	Angle of rotation about x-axis
θ_p	Angle defined in text
ϕ	Angle of rotation about z-axis
ϕ_p	Angle defined in text
Φ^+	Angle defined in text
Φ^-	Angle defined in text
ψ_1	Angle defined in text
ψ^2	Angle defined in text
Ψ	Angle defined in text
σ	Electrical conductivity (S/m)

Subscripts and Superscripts

l	Liquid
max	Maximum value
n	Corresponding to increment n
s	Solid
S	Series
–	Mean value

REFERENCES

BRAILSFORD, A.D. and MAJOR, K.G. 1964. The thermal conductivity of aggregates of several phases including porous materials. Brit. J. Appl. Phys. *15*, 313-319.

DE ALWIS, A.A.P. and FRYER, P.J. 1990. A finite element analysis of heat generation and transfer during ohmic heating of food. Chem. Eng. Sci. *45*(6), 1547–1559.

KOPELMAN, I.J. 1966. Transient heat transfer and thermal properties in food systems. Ph.D. Dissertation, Michigan State University, East Lansing, MI.

MAXWELL, J.C. 1881. *A Treatise on Electricity and Magnetism, Vol. 1*, 2nd ed., Clarendon Press, Oxford, England.

MEREDITH, R.E. and TOBIAS, C.W. 1960. Resistance to potential flow through a cubical array of spheres. J. Applied Phys. *31*, 1270–73.

PALANIAPPAN, S. and SASTRY, S.K. 1991. Modeling of electrical conductivity of liquid-particle mixtures. Food and Bioproducts Proc., Part C. Trans. Instn. Chem. Engrs. (UK), *69*, 167–174.

F N P

PUBLICATIONS IN FOOD SCIENCE AND NUTRITION

Journals

JOURNAL OF FOOD LIPIDS, F. Shahidi
JOURNAL OF RAPID METHODS AND AUTOMATION IN MICROBIOLOGY, D.Y.C. Fung and M.C. Goldschmidt
JOURNAL OF MUSCLE FOODS, N.G. Marriott and G.J. Flick, Jr.
JOURNAL OF SENSORY STUDIES, M.C. Gacula, Jr.
JOURNAL OF FOODSERVICE SYSTEMS, C.A. Sawyer
JOURNAL OF FOOD BIOCHEMISTRY, J.R. Whitaker, N.F. Haard and H. Swaisgood
JOURNAL OF FOOD PROCESS ENGINEERING, D.R. Heldman and R.P. Singh
JOURNAL OF FOOD PROCESSING AND PRESERVATION, D.B. Lund
JOURNAL OF FOOD QUALITY, J.J. Powers
JOURNAL OF FOOD SAFETY, T.J. Montville and A.J. Miller
JOURNAL OF TEXTURE STUDIES, M.C. Bourne and P. Sherman

Books

MICROWAVE FOODS: NEW PRODUCT DEVELOPMENT, R.V. Decareau
DESIGN AND ANALYSIS OF SENSORY OPTIMIZATION, M.C. Gacula, Jr.
NUTRIENT ADDITIONS TO FOOD, J.C. Bauernfeind and P.A. Lachance
NITRITE-CURED MEAT, R.G. Cassens
THE POTENTIAL FOR NUTRITIONAL MODULATION OF THE AGING PROCESSES, D.K. Ingram *et al.*
CONTROLLED/MODIFIED ATMOSPHERE/VACUUM PACKAGING OF FOODS, A.L. Brody
NUTRITIONAL STATUS ASSESSMENT OF THE INDIVIDUAL, G.E. Livingston
QUALITY ASSURANCE OF FOODS, J.E. Stauffer
THE SCIENCE OF MEAT AND MEAT PRODUCTS, 3RD ED., J.F. Price and B.S. Schweigert
HANDBOOK OF FOOD COLORANT PATENTS, F.J. Francis
ROLE OF CHEMISTRY IN THE QUALITY OF PROCESSED FOODS, O.R. Fennema, W.H. Chang and C.Y. Lii
NEW DIRECTIONS FOR PRODUCT TESTING AND SENSORY ANALYSIS OF FOODS, H.R. Moskowitz
PRODUCT TESTING AND SENSORY EVALUATION OF FOODS, H.R. Moskowitz
ENVIRONMENTAL ASPECTS OF CANCER: ROLE OF MACRO AND MICRO COMPONENTS OF FOODS, E.L. Wynder *et al.*
FOOD PRODUCT DEVELOPMENT IN IMPLEMENTING DIETARY GUIDELINES, G.E. Livingston, R.J. Moshy, and C.M. Chang
SHELF-LIFE DATING OF FOODS, T.P. Labuza
ANTINUTRIENTS AND NATURAL TOXICANTS IN FOOD, R.L. Ory
UTILIZATION OF PROTEIN RESOURCES, D.W. Stanley *et al.*
VITAMIN B_6: METABOLISM AND ROLE IN GROWTH, G.P. Tryfiates
POSTHARVEST BIOLOGY AND BIOTECHNOLOGY, H.O. Hultin and M. Milner

Newsletters

MICROWAVES AND FOOD, R.V. Decareau
FOOD INDUSTRY REPORT, G.C. Melson
FOOD, NUTRITION AND HEALTH, P.A. Lachance and M.C. Fisher
FOOD PACKAGING AND LABELING, S. Sacharow

GUIDE FOR AUTHORS

Typewritten manuscripts in triplicate should be submitted to the editorial office. The typing should be double-spaced throughout with one-inch margins on all sides.

Page one should contain: the title, which should be concise and informative; the complete name(s) of the author(s); affiliation of the author(s); a running title of 40 characters or less; and the name and mail address to whom correspondence should be sent.

Page two should contain an abstract of not more than 150 words. This abstract should be intelligible by itself.

The main text should begin on page three and will ordinarily have the following arrangement:

Introduction: This should be brief and state the reason for the work in relation to the field. It should indicate what new contribution is made by the work described.

Materials and Methods: Enough information should be provided to allow other investigators to repeat the work. Avoid repeating the details of procedures which have already been published elsewhere.

Results: The results should be presented as concisely as possible. Do not use tables *and* figures for presentation of the same data.

Discussion: The discussion section should be used for the interpretation of results. The results should not be repeated.

In some cases it might be desirable to combine results and discussion sections.

References: References should be given in the text by the surname of the authors and the year. *Et al.* should be used in the text when there are more than two authors. All authors should be given in the Reference section. In the Reference section the references should be listed alphabetically. See below for style to be used.

DEWALD, B., DULANEY, J.T., and TOUSTER, O. 1974. Solubilization and polyacrylamide gel electrophoresis of membrane enzymes with detergents. In *Methods in Enzymology,* Vol. xxxii, (S. Fleischer and L. Packer, eds.) pp. 82–91, Academic Press, New York.

HASSON, E.P. and LATIES, G.G. 1976. Separation and characterization of potato lipid acylhydrolases. Plant Physiol. *57,*142–147.

ZABORSKY, O. 1973. *Immobilized Enzymes,* pp. 28–46, CRC Press, Cleveland, Ohio.

Journal abbreviations should follow those used in *Chemical Abstracts.* Responsibility for the accuracy of citations rests entirely with the author(s). References to papers in press should indicate the name of the journal and should only be used for papers that have been accepted for publication. Submitted papers should be referred to by such terms as "unpublished observations" or "private communication." However, these last should be used only when absolutely necessary.

Tables should be numbered consecutively with Arabic numerals. The title of the table should appear as below:

Table 1. Activity of potato acyl-hydrolases on neutral lipids, galactolipids, and phospholipids

Description of experimental work or explanation of symbols should go below the table proper. Type tables neatly and correctly as tables are considered art and are not typeset. Single-space tables.

Figures should be listed in order in the text using Arabic numbers. Figure legends should be typed on a separate page. Figures and tables should be intelligible without reference to the text. Authors should indicate where the tables and figures should be placed in the text. Photographs must be supplied as glossy black and white prints. Line diagrams should be drawn with black waterproof ink on white paper or board. The lettering should be of such a size that it is easily legible after reduction. Each diagram and photograph should be clearly labeled on the reverse side with the name(s) of author(s), and title of paper. When not obvious, each photograph and diagram should be labeled on the back to show the top of the photograph or diagram.

Acknowledgments: Acknowledgments should be listed on a separate page.

Short notes will be published where the information is deemed sufficiently important to warrant rapid publication. The format for short papers may be similar to that for regular papers but more concisely written. Short notes may be of a less general nature and written principally for specialists in the particular area with which the manuscript is dealing. Manuscripts which do not meet the requirement of importance and necessity for rapid publication will, after notification of the author(s), be treated as regular papers. Regular papers may be very short.

Standard nomenclature as used in the engineering literature should be followed. Avoid laboratory jargon. If abbreviations or trade names are used, define the material or compound the first time that it is mentioned.

EDITORIAL OFFICES: DR. D.R. HELDMAN, COEDITOR, *Journal of Food Process Engineering,* Weinberg Consulting Group Inc., 1220 19th St., N.W., Washington, D.C. 20036 USA; or DR. R.P. SINGH, COEDITOR, *Journal of Food Process Engineering,* University of California, Davis, Department of Agricultural Engineering, Davis, CA 95616 USA.

JOURNAL OF FOOD PROCESS ENGINEERING VOL. 15, NO. 3

CONTENTS